

Testing Gluon Self-Interactions in Three Jet Events at Hadron Colliders^{*}

Lance Dixon and Yael Shadmi

*Stanford Linear Accelerator Center
Stanford, CA 94309*

Abstract

The effective operator $\text{tr}(G^3)$ is the only dimension-6 gluonic operator that cannot be related to four-quark operators. A peculiar property of this operator is that it does not contribute to two-jet production at hadron colliders, at the level of one operator insertion and leading-order in α_s ; therefore we study its effects on three jet events. To calculate the helicity amplitudes induced by this operator we make extensive use of collinear factorization. We propose several ways of detecting the $\text{tr}(G^3)$ signal, one of which exploits its non-trivial behavior under azimuthal rotations of two almost collinear jets.

Submitted to Nuclear Physics B

^{*}Research supported by the Department of Energy under grant DE-AC03-76SF00515.

1. Introduction

The gluon self-coupling is perhaps the clearest manifestation of the non-abelian nature of QCD. Tests of QCD are therefore incomplete without quantitative tests of the gluonic sector. New physics which respects the symmetries of QCD can produce deviations from the QCD prediction for the gluon self-coupling at higher energies. The deviations can be parametrized by an effective Lagrangian including higher-dimension operators which describe the low-energy effects of the new physics. By calculating the effect of these operators on partonic scattering, one can set lower bounds on the characteristic energy scale, Λ , of the new physics in a manner independent of the details of the new physics.

The use of higher dimension operators as probes for new physics was originally suggested for interactions of leptons and quarks [1]. In the quark case, the dimension-6 operators are four-quark contact operators and they affect $2 \rightarrow 2$ quark scattering ($q\bar{q} \rightarrow q\bar{q}$ etc.) at leading-order. Measurements of the dijet invariant mass distribution at 1.8 TeV by the CDF collaboration have recently led to a bound of 1.3 TeV on the scale Λ associated with such operators [2], where Λ is defined by the conventions of ref. [1].

This approach was first applied to testing purely gluonic interactions by Simmons in ref. [3]. It turns out, for reasons we will discuss in the following, that placing bounds on the scale of deviations from QCD in the gluon sector is more difficult than in the quark sector. It is this difficulty which the present work addresses. Though most previous work has concentrated on the two-jet cross-section, we will argue here that the gluonic dimension-6 operator $\text{tr}(G^3)$ can be bounded most efficiently by studying three jet events at hadron colliders.

To test the gluon sector of QCD quantitatively, an effective Lagrangian that preserves the main features of QCD is desirable. At the level of dimension-6 operators the unique effective Lagrangian that can be constructed from gluon fields alone, and that is $SU(3)$ gauge-invariant and CP-even is [3]

$$\mathcal{L}_{\text{eff}} = \mathcal{L}_{\text{QCD}} + C \frac{g_s}{\Lambda^2} f_{abc} G_\nu^{a\mu} G_\rho^{b\nu} G_\mu^{c\rho} + C' \frac{1}{\Lambda'^2} D_\mu G_\nu^{a\mu} D_\rho G^{a\rho\nu}, \quad (1)$$

where $G_{\mu\nu} = -(i/g_s)[D_\mu, D_\nu]$ is the gluon field strength, $D_\mu = \partial_\mu + ig_s A_\mu$ is the covariant derivative, Λ and Λ' are the characteristic energy scales of the new physics and C and C' are numerical coefficients. In accord with the conventions of ref. [1], we take $C = C' = 4\pi$; then this equation defines Λ and Λ' .

The new physics could be associated with heavy colored particles which couple to gluons and affect their interactions through loops, in which case the scales Λ , Λ' would be proportional to the mass of the heavy particle, with a proportionality factor that depends on the details of the new physics, such as the spin and color of the heavy particle.

Alternatively, the new physics could be gluon compositeness, in which case Λ , Λ' would be proportional to the scale of the interaction between the gluon constituents. In this work we do not concern ourselves with the possible source of new physics, but rather discuss the implications of the effective Lagrangian (1) as a model-independent test of gluon self-interactions.

Using the equation of motion for the gluon field A_μ , the second operator in (1) can be written as a four-quark contact operator [3]. Thus, it cannot provide a clean test of the gluon sector independently of quark effects. Also, since this operator is equivalent to a four-quark operator, it is fairly easy to obtain a good bound on the scale Λ associated with it just as in the case of four-quark operators; Simmons and Cho have recently estimated this bound as 2.03 TeV [4].

In the following we will therefore neglect the second operator in (1) (i.e., we set $\Lambda' = \infty$), as well as four-quark operators, and focus on the first operator in (1), to which we refer as $\text{tr}(G^3)$.

Unfortunately, unlike the four-quark contact operators which interfere with pure QCD at leading-order in α_s and in $1/\Lambda^2$, the leading-order contribution of $\text{tr}(G^3)$ to massless-parton scattering vanishes: the four-parton tree amplitudes containing one insertion of this operator have a helicity structure which is orthogonal to that of four-parton QCD tree amplitudes when the four partons are massless [3]. A leading order contribution from $\text{tr}(G^3)$ does appear in four jet decays of the Z-boson, as discussed by Duff and Zeppenfeld [5], but because of their small center-of-mass energy these processes are only sensitive to scales Λ around 100 GeV, which is low compared to the typical energy scales of scattering processes in hadron colliders. Therefore, in order to obtain good bounds on the scale of $\text{tr}(G^3)$ it is necessary to compute its effect on processes in hadron colliders at the next order, either in $1/\Lambda^2$ or in α_s .

The former option was pursued by Simmons [3], and later by Dreiner *et al.* [6]. Simmons studied the effect of the gluonic operator on $2 \rightarrow 2$ parton scattering ($gg \rightarrow gg$, $q\bar{q} \rightarrow gg$, $q\bar{q} \rightarrow q\bar{q}$ and processes related by crossing symmetry) at order $1/\Lambda^4$. Such contributions come either from squaring amplitudes with one insertion of $\text{tr}(G^3)$, or from interfering QCD amplitudes with amplitudes containing two insertions of $\text{tr}(G^3)$. The main feature of this correction as seen in dijet production, or alternatively, in inclusive jet production in hadron colliders, is an excess of events in the high p_T region of the jet transverse-momentum (p_T) distribution. This signal roughly grows as $(\hat{s}/\Lambda^2)^2$ where \hat{s} is the parton center-of-mass energy. It is therefore highly suppressed at low energies, and becomes appreciable only at energies of the order of Λ , where unitarity is violated, and where the parametrization in terms of the effective operator $\text{tr}(G^3)$ can no longer be

trusted [6]. Including a form-factor to unitarize the cross-section reduces the $\text{tr}(G^3)$ signal at high energies dramatically, leading to deviations from QCD that are on the order of the theoretical and experimental uncertainties [6].

An additional drawback of this approach is that at the order $1/\Lambda^4$ contributions from dimension-8 operators must be included as well. Since there are many such dimension-8 operators [3], it is very hard to treat the problem in full generality.

The difficulties encountered here are related to the fact that the contribution studied is $O(1/\Lambda^4)$. It seems desirable therefore to investigate the leading-order contribution in $1/\Lambda^2$, while going to higher order in α_s . In this case there are several options to consider. The first is to study the effect of the gluonic operator on *inclusive* jet production in hadron colliders at order $1/\Lambda^2$ and next-to-leading order in α_s . Three types of contributions appear at this order. The first is the interference of $2 \rightarrow 2$ tree amplitudes containing one insertion of the gluonic operator, with $2 \rightarrow 2$ QCD *loop* amplitudes. This contribution is easy to obtain since the relevant QCD loop helicity amplitudes have been calculated using both string techniques [7] and Feynman diagrams [8], and the helicity amplitudes containing one insertion of the gluonic operator are readily calculable with the use of the helicity basis. The second contribution involves the interference of QCD $2 \rightarrow 2$ tree amplitudes with *loop* amplitudes containing one insertion of the gluonic operator. The latter amplitudes are hard to compute. Finally, the third contribution arises from the interference of QCD $2 \rightarrow 3$ tree amplitudes ($gg \rightarrow ggg$, $gg \rightarrow q\bar{q}g$, $q\bar{q} \rightarrow q\bar{q}g$ and processes related by crossing symmetry) with $2 \rightarrow 3$ tree amplitudes containing one insertion of the gluonic operator.

In addition to the technical difficulty of calculating the second contribution, this approach suffers from a more serious problem. A rough estimate of the order of magnitude of (i) the QCD cross-section, (ii) the correction calculated by Simmons ($O(1/\Lambda^4)$), and (iii) the $O(1/\Lambda^2)$ correction suggested above, reveals that the $O(1/\Lambda^2)$ correction only dominates over the $O(1/\Lambda^4)$ correction at low energies, where they are both insignificant compared to QCD. This is largely due to a factor of $\alpha_s/(4\pi)$ suppressing the loop amplitudes. Instead, in this work we use the third contribution mentioned above, namely the interference of QCD $2 \rightarrow 3$ tree amplitudes with $2 \rightarrow 3$ tree amplitudes containing one insertion of the gluonic operator, in order to probe the gluonic operator through *exclusive three jet* production in hadron colliders. In three-jet production, the $\text{tr}(G^3)$ correction is a leading order correction, both in $1/\Lambda^2$ and in α_s .

The use of three jet events in hadron colliders to test QCD has been discussed in the past [9,10]. Here we propose three different ways for studying the $\text{tr}(G^3)$ signal in three jet events. The first involves the region in which the three jets are well separated, the second involves the region in which two of the jets are almost collinear, and the third involves the

cross-over between these two regions. The first approach is probably the easiest one from the point of view of the experiment but it leads to smaller $\text{tr}(G^3)$ signals.

The second approach is perhaps the most interesting from a theoretical point of view. In the region in which two of the partons are almost collinear, we use a special angular dependence of the $\text{tr}(G^3)$ signal to isolate it from QCD. We discuss this approach in detail in section 3 and section 4 but we briefly outline the idea here. When two of the partons are almost collinear the three-jet event looks almost like a two-jet event, where one of the partons has a momentum p which is the sum of the two collinear momenta. The QCD cross-section and the $\text{tr}(G^3)$ correction to it have different properties under azimuthal rotations of the collinear momenta around p , with p held fixed. An azimuthal dependence of the cross-section in the collinear region requires a linear polarization of the “effective gluon” which replaces the two collinear gluons in the resulting four-parton cross-section. However, a consequence of the supersymmetric Ward identities (SWI) [11,12,13] is that two of the three independent four-gluon helicity amplitudes, and one of the two independent two-quark two-gluon amplitudes vanish for tree-level QCD. It follows that for fixed helicities of the five external partons there is only one possible effective gluon helicity; it cannot be linearly polarized, and so the tree-level QCD cross-section has no dependence on azimuthal rotations of two collinear partons. On the other hand, after adding the $\text{tr}(G^3)$ -induced amplitude, both helicities contribute, giving rise to a linear polarization of the effective gluon and a characteristic azimuthal dependence of the cross-section. Precisely the same orthogonality of the helicity structures of the QCD and the $\text{tr}(G^3)$ -induced four-parton amplitudes, which prevents the appearance of the $\text{tr}(G^3)$ signal at leading-order, also causes these different behaviors in the collinear region, thus providing a means for separating the $\text{tr}(G^3)$ signal from the QCD background. In measuring the azimuthal dependence of the collinear three-jet cross-section, one simultaneously probes for the existence of the $\text{tr}(G^3)$ operator, and tests the helicity structure of QCD and thereby the supersymmetric Ward identities.

As is well known, the calculation of QCD amplitudes is not a trivial task. This task becomes even more daunting with the inclusion of the gluonic dimension-6 operator, which leads to cumbersome vertices for three-gluon, four-gluon and five-gluon couplings, all of which would be needed here. It is therefore crucial to use methods which simplify the calculation. This work illustrates the power of several such tools, namely, color ordering [14] the helicity basis [15, 16], and collinear factorization [17,16] for this extension of QCD. Thus for example, the orthogonality of QCD amplitudes and amplitudes induced by the gluonic operator at lowest order is immediately derived and becomes very transparent using the helicity basis. Calculating the new five-gluon vertex becomes unnecessary since we can infer

the five-parton amplitudes from the four-parton amplitudes using collinear factorization. For some of the calculations we can extract the contribution of the effective operator by thinking of it as induced by a heavy colored particle in the loop, taking advantage of existing string-based QCD loop calculations [7,18].

This paper is organized as follows: in section 2 we explain our notation and discuss the calculation of the new amplitudes. We give analytic expressions for the new four-parton and five-parton amplitudes, and for the corrections to the cross-section at the parton level. We discuss the behavior of these corrections in the soft and collinear regions of phase space in section 3. We then go on to describe the hadron-level calculation, and suggest different ways of looking for the $\text{tr}(G^3)$ signal in three jet events in section 4. We conclude with a summary of the results in section 5. The appendix reviews properties of color-ordered amplitudes and collinear factorization, and shows that $\text{tr}(G^3)$ does not induce any collinear singularities on top of the QCD singularities.

2. Calculating the new amplitudes and interference terms

The operator $\text{tr}(G^3)$ induces new three-, four-, five- and six-gluon vertices. The three-gluon vertex has the same power of the strong coupling, g_s , as the QCD vertex, and the other new vertices acquire an additional factor g_s with each additional gluon. All the new vertices have $1/\Lambda^2$ multiplying them. To compute the effect of $\text{tr}(G^3)$ on three-jet production in hadron-colliders, one needs to evaluate five-parton tree amplitudes with one insertion of the new operator, i.e., one new three-, four- or five-gluon vertex. We denote these new amplitudes by the super-script (Λ).

We now briefly describe our notation and the methods used to organize the calculation: color ordering, the helicity basis and collinear factorization. In this we follow closely the review by Mangano and Parke [16].

Tree amplitudes of $SU(N)$ gauge theories can be organized in a simple color basis [16]. Each amplitude is written as a sum of color factors multiplied by color sub-amplitudes which correspond to specific color-orderings. Since all the color dependence is factored out of the sub-amplitudes, and since the color basis is orthogonal at leading order in the number of colors, each sub-amplitude is separately gauge invariant and can be calculated using any gauge choice. The n -gluon amplitude \mathcal{A}_n can be written as,

$$\mathcal{A}_n = \sum_{\{12..n\}'} \text{tr}(T^{a_1} T^{a_2} \dots T^{a_n}) A_n(1, 2, \dots, n) . \quad (2)$$

Here $A_n(1, 2, \dots, n) = A_n(p_1, \lambda_1; p_2, \lambda_2; \dots; p_n, \lambda_n)$ and p_i, λ_i are the momentum and helicity of the i -th gluon. The sum in (2) is over non-cyclic permutations of $\{1, 2, \dots, n\}$. We

discuss some useful properties of the color sub-amplitudes in the appendix.

Amplitudes with n gluons and one quark pair can be written as,

$$\mathcal{A}_n = \sum_{\{12..n\}} (T^{a_1} T^{a_2} \dots T^{a_n})_{i\bar{j}} A_n(q; 1, 2, \dots, n; \bar{q}) . \quad (3)$$

Here $A_n(q; 1, 2, \dots, n; \bar{q}) = A_n(q^\lambda; p_1, \lambda_1; p_2, \lambda_2; \dots; p_n, \lambda_n; \bar{q}^{\bar{\lambda}})$, q, λ are the quark momentum and helicity, $\bar{q}, \bar{\lambda}$ are the anti-quark momentum and helicity, p_i, λ_i are the momentum and helicity of the i -th gluon, and the sum is over all permutations of the n gluons.

We will also need amplitudes with two quark pairs and one gluon. These we write as,

$$\begin{aligned} \mathcal{A}_5 = & A_5(q_1, \bar{q}_1; q_2, \bar{q}_2; k) \frac{1}{N} \delta_{i_1 \bar{i}_1} T_{i_2 \bar{i}_2}^a + A_5(q_1, \bar{q}_2; q_2, \bar{q}_1; k) \delta_{i_1 \bar{i}_2} T_{i_2 \bar{i}_1}^a + \\ & + A_5(q_2, \bar{q}_2; q_1, \bar{q}_1; k) \frac{1}{N} \delta_{i_2 \bar{i}_2} T_{i_1 \bar{i}_1}^a + A_5(q_2, \bar{q}_1; q_1, \bar{q}_2; k) \delta_{i_2 \bar{i}_1} T_{i_1 \bar{i}_2}^a , \end{aligned} \quad (4)$$

where q_i, \bar{q}_i are the momenta of the i -th quark and anti-quark, and k is the gluon momentum.

Calculating the new amplitudes is greatly simplified by using the helicity basis [15,16]. Each gluon polarization is represented in terms of the gluon momentum and another light-like momentum, the reference momentum. Choosing the reference momentum as an appropriate combination of the external momenta (this choice can be made separately for different color sub-amplitudes) results in many cancellations in the calculation. With this representation of the polarization vectors, helicity amplitudes of massless external partons are naturally expressed in terms of spinor products, which are nothing but square roots of the Lorentz invariants up to phases. The spinor products are denoted as:

$$\begin{aligned} [i j] &\equiv \langle i+ | j- \rangle = \bar{u}_+(k_i) u_-(k_j) , \\ \langle i j \rangle &\equiv \langle i- | j+ \rangle = \bar{u}_-(k_i) u_+(k_j) , \end{aligned} \quad (5)$$

where $|i+\rangle$ ($|i-\rangle$) is a positive (negative) helicity spinor with the momentum of parton i . We give an explicit representation of the spinor-products in the appendix.

One of the useful properties of color-ordered helicity amplitudes is their factorization on collinear poles. When the color adjacent partons $i, i+1$, with momenta k_i, k_{i+1} become collinear, the n -parton color sub-amplitude factorizes on the $(n-1)$ -parton color sub-amplitudes where the two collinear partons are replaced by one parton with momentum $p = k_i + k_{i+1}$ and with positive or negative helicity. We sometimes refer to this parton as the effective parton. Except for a subtlety in the terms sub-leading in the number of colors in the four-quark one-gluon amplitudes (discussed below), each n -parton color structure

factorizes on a unique $(n - 1)$ -parton color structure. In the collinear limit $k_i = zp$, $k_{i+1} = (1 - z)p$ and [17,16],

$$A_n(k_1, \dots, k_i, k_{i+1}, \dots, k_n) \rightarrow^{i||i+1} \sum_{\lambda=\pm} \text{Split}_{-\lambda}(i, i + 1) A_{n-1}(k_1, \dots, (k_i+k_{i+1})^\lambda, \dots, k_n). \quad (6)$$

The splitting function $\text{Split}_{-\lambda}(i, j)$ depends on the helicity λ of the effective parton, on the helicities of the two collinear partons and on the momentum fraction z , and is singular as $s_{i,i+1} = (k_i + k_{i+1})^2 \rightarrow 0$. The splitting functions are analogues of the Altarelli-Parisi coefficients [19] that are associated with color-ordered helicity amplitudes instead of cross-sections. Specifically, the absolute value of the splitting-function, squared and color-averaged, is equal to the appropriate polarized Altarelli-Parisi coefficient. We list the relevant splitting functions in the appendix.

Amplitudes with insertions of $\text{tr}(G^3)$ satisfy (6) as well. When the two collinear gluons i, j are attached to the new three-gluon vertex, one can show (see appendix) that the expression for this vertex goes to zero at least as fast as s_{ij} , cancelling the $1/s_{ij}$ propagator pole. This is related to the fact that the new vertex has extra powers of momenta in the numerator compared to the QCD vertex, to compensate for $1/\Lambda^2$. Thus the only splitting functions which occur for the five-parton new amplitudes are the standard splitting functions arising from the QCD vertices and so,

$$A_n^{(\Lambda)}(k_1, \dots, k_i, k_{i+1}, \dots, k_n) \rightarrow^{i||i+1} \sum_{\lambda=\pm} \text{Split}_{-\lambda}(i, i + 1) A_{n-1}^{(\Lambda)}(k_1, \dots, (k_i+k_{i+1})^\lambda, \dots, k_n). \quad (7)$$

Collinear factorization provides a check of n -parton amplitudes when the $(n - 1)$ -parton amplitudes are known. Moreover, it is often possible to infer the former from the latter [20]. In this work we calculate the relevant $\text{tr}(G^3)$ -corrected four-parton amplitudes and then guess the form of the five-parton amplitudes by requiring that they have the correct behavior in all collinear limits. There could be, however, additional terms in the amplitudes which are finite in all the collinear limits. We have not been able to find any such terms that also have the correct dimension and for the five-gluon amplitudes also satisfy the $U(1)$ decoupling equation (see the appendix). Still, to verify the results obtained from collinear factorization, we calculated at least one helicity amplitude for each case (5-gluon, 2-quarks 3-gluons, and 4-quarks 1-gluon) using an alternative method. We find agreement with the results obtained from collinear factorization; there are no additional finite terms which are missed when collinear factorization is used to infer the five-parton $\text{tr}(G^3)$ amplitudes.

We begin by listing the relevant four-parton amplitudes. These are obtained from Feynman diagrams using the helicity basis, and can be written as one-term expressions.

For the four helicity amplitudes in $gg \rightarrow gg$ we have, with $g_s = 1$,

$$\begin{aligned}
A_4^{(\Lambda)}(1^+, 2^+, 3^+, 4^+) &= \frac{3i}{\Lambda^2} \frac{2s_{12}s_{23}s_{13}}{\langle 12 \rangle \langle 23 \rangle \langle 34 \rangle \langle 41 \rangle} , \\
A_4^{(\Lambda)}(1^-, 2^+, 3^+, 4^+) &= \frac{3i}{\Lambda^2} \frac{-[23]^2[34]^2[42]^2}{[12][23][34][41]} , \\
A_4^{(\Lambda)}(1^-, 2^-, 3^+, 4^+) &= 0 , \\
A_4^{(\Lambda)}(1^-, 2^+, 3^-, 4^+) &= 0 .
\end{aligned} \tag{8}$$

The corresponding $gg \rightarrow gg$ QCD tree amplitudes are:

$$\begin{aligned}
A_4(1^+, 2^+, 3^+, 4^+) &= 0 , \\
A_4(1^-, 2^+, 3^+, 4^+) &= 0 , \\
A_4(1^+, 2^+, 3^-, 4^-) &= A_4(1^+, 2^-, 3^+, 4^-) = i \frac{\langle 34 \rangle^4}{\langle 12 \rangle \langle 23 \rangle \langle 34 \rangle \langle 41 \rangle} .
\end{aligned} \tag{9}$$

Comparing (8) and (9) it is easy to see that the interference vanishes, and there is no $\text{tr}(G^3)$ induced correction at leading order. Similarly, for $qg \rightarrow qg$,

$$\begin{aligned}
A_4^{(\Lambda)}(q^+; 1^+, 2^+; \bar{q}^-) &= \frac{3i}{\Lambda^2} \frac{[12]^2[q1]^2[\bar{q}2][2q]}{[\bar{q}q][q1][12][2\bar{q}]} , \\
A_4^{(\Lambda)}(q^-; 1^+, 2^+; \bar{q}^+) &= \frac{3i}{\Lambda^2} \frac{-[12]^2[\bar{q}2]^2[q1][1\bar{q}]}{[\bar{q}q][q1][12][2\bar{q}]} , \\
A_4^{(\Lambda)}(q^+; 1^+, 2^-; \bar{q}^-) &= 0 , \\
A_4^{(\Lambda)}(q^-; 1^+, 2^+; \bar{q}^+) &= 0 .
\end{aligned} \tag{10}$$

The $qg \rightarrow qg$ QCD tree amplitudes are:

$$\begin{aligned}
A_4(q^+; 1^+, 2^+; \bar{q}^-) &= 0 , \\
A_4(q^-; 1^+, 2^+; \bar{q}^+) &= 0 , \\
A_4(q^+; 1, 2; \bar{q}^-) &= i \frac{-\langle \bar{q}i \rangle^3 \langle qi \rangle}{\langle \bar{q}q \rangle \langle q1 \rangle \langle 12 \rangle \langle 2\bar{q} \rangle} , \\
A_4(q^-; 1, 2; \bar{q}^+) &= i \frac{\langle qi \rangle^3 \langle \bar{q}i \rangle}{\langle \bar{q}q \rangle \langle q1 \rangle \langle 12 \rangle \langle 2\bar{q} \rangle} ,
\end{aligned} \tag{11}$$

where i is the negative helicity gluon and again there is no leading-order interference.

An alternative way to obtain the amplitudes in (8) and (10), is to think of the operator $\text{tr}(G^3)$ as being induced by a heavy colored scalar of mass M_s on the order of Λ , circulating

in a loop, and to calculate the $1/M_s^2$ term in the resulting loop amplitude. This is not as cumbersome as it may seem, since all the relevant loop amplitudes have been calculated by Bern and Kosower [7] using string techniques for the case of a massless particle in the loop. The Feynman parameter polynomials for a massive scalar are identical to those for a massless scalar, since the derivative interactions are identical. Only the scalar denominator of the Feynman integral is changed. In the limit of large M_s , the only $O(1/M_s^2)$ contributions come from the triangle diagrams, i.e., diagrams with three legs attached to the loop. The resulting Feynman parameter integrations are simply integrations over polynomials. Subtleties of ultraviolet and infrared divergences and coupling-constant shifts, do not occur in these loop amplitudes because the corresponding QCD tree amplitudes vanish. By calculating $A_4^{(\Lambda)}(q^+; 3^+, 4^+; \bar{q}^-)$ in both ways, we extract the ratio between M_s and Λ , $\Lambda^2 = 720\pi M_s^2/\alpha_s$. We then use this ratio to check that the two methods agree for the remaining amplitudes.

The zeroes in equations (9) and (11) are manifestations of the supersymmetric Ward identities (SWI) [11,12] (unlike the zeroes in equations (8) and (10), whose origin is obscure). According to these identities, the only non-vanishing four-parton amplitudes are the ones with two positive and two negative parton helicities. For QCD, which is not supersymmetric, the SWI are satisfied at tree-level only [13]. Because of the SWI, as we will see in the following, the five-parton tree-level QCD cross-section is invariant under azimuthal rotations of two collinear partons which leave the sum of the collinear momenta fixed.

We now turn our attention to the five-parton amplitudes. Since we are interested in the interference of $\text{tr}(G^3)$ -induced amplitudes with QCD tree amplitudes, we have to calculate only the new amplitudes corresponding to helicity choices for which the QCD tree amplitudes are non-zero. These are $(+++--)$ and $(++-+-)$ for the five-gluon amplitudes, $(\pm; ++-; \mp)$, $(\pm; +-+; \mp)$ and $(\pm; -++; \mp)$ for the two-quark-three-gluon amplitudes, and all possible helicity structures for the four-quark-one-gluon amplitudes.

To illustrate the use of collinear factorization in deriving these amplitudes, consider the 2-quark 3-gluon amplitude $A_5^{(\Lambda)}(q^+; 1^+, 2^+, 3^-; \bar{q}^-)$. In the limit when q and k_1 become collinear, this amplitude should factorize on the 4-parton amplitude $A_4^{(\Lambda)}(p^+; 2^+, 3^-; \bar{q}^-)$ with $p = q + k_1$. Since the latter amplitude is zero, $A_5^{(\Lambda)}(q^+; 1^+, 2^+, 3^-; \bar{q}^-)$ cannot be singular in this limit. Similarly, it remains finite as gluons 1 and 2 become collinear because $\text{Split}_+(+, +)$ is zero (see the appendix). However, in the limit where gluons 2 and

3 are collinear with $k_2 = zp$ and $k_3 = (1 - z)p$,

$$\begin{aligned} A_5^{(\Lambda)}(q^+; 1^+, 2^+, 3^-; \bar{q}^-) &\simeq \text{Split}_-(2^+, 3^-) \times A_4^{(\Lambda)}(q^+; 1^+, p^+; \bar{q}^-) \\ &= \frac{z^{3/2}}{(1 - z)^{1/2} [23]} 3i \frac{1}{\Lambda^2} \frac{[1p][1q][pq]}{[\bar{q}q]} . \end{aligned}$$

This is satisfied by the expression

$$A_5^{(\Lambda)}(q^+; 1^+, 2^+, 3^-; \bar{q}^-) = 3i \frac{1}{\Lambda^2} \frac{[2\bar{q}][1q][12][2q]}{[\bar{q}q][23][3\bar{q}]} ,$$

which also has the correct behavior when \bar{q} and k_3 , and \bar{q} and q become collinear, and which agrees with the result obtained from a Feynman diagram calculation.

In tree amplitudes with zero or one quark pair, the n -parton color sub-amplitude always factorizes on a unique $(n - 1)$ -parton sub-amplitude. The situation is slightly different for amplitudes with two quark pairs, where the color ordering is not unique at subleading order in the number of colors. Thus for example as q_1 and \bar{q}_2 become collinear in the $O(1/N_c)$ sub-amplitude $A^{(\Lambda)}(q_1, \bar{q}_1; q_2, \bar{q}_2; k)$ there are contributions from both orderings of the two gluons (the original gluon and the one replacing the pair q_1, \bar{q}_1) attached to the remaining quark line. Thus one finds,

$$A^{(\Lambda)}(q_1, \bar{q}_1; q_2, \bar{q}_2; k) \simeq \text{Split}_+(\bar{q}_1, q_1)(A(q_2; k, p; \bar{q}_2) + A(q_2; p, k; \bar{q}_2)) .$$

Our results for the $\text{tr}(G^3)$ -induced five-parton amplitudes are as follows.

For $gg \rightarrow ggg$,

$$A_5^{(\Lambda)}(i^+, j^+, k^+, l^-, m^-) = \frac{3i}{\Lambda^2} \frac{[ij]^2[jk]^2[ki]^2}{[12][23][34][45][51]} , \quad (12)$$

where l^- and m^- are not necessarily adjacent. This expression was inferred from collinear factorization. As a check, we modified the string-based calculations of five-gluon loop amplitudes with a massless scalar in the loop [18] to obtain the $1/M_s^2$ contribution from a scalar of mass M_s , which agreed with equation (12).

The $gg \rightarrow ggg$ QCD tree amplitude which interferes with (12) is:

$$A_5(i^+, j^+, k^+, l^-, m^-) = i \frac{\langle lm \rangle^4}{\langle 12 \rangle \langle 23 \rangle \langle 34 \rangle \langle 45 \rangle \langle 51 \rangle} , \quad (13)$$

where, as in (12), l and m are not necessarily adjacent.

For the two-quark three-gluon amplitudes we find,

$$A_5^{(\Lambda)}(q^+; 1, 2, 3; \bar{q}^-) = \frac{3i}{\Lambda^2} \frac{-[ij]^2[qi]^2[jq][\bar{q}j]}{[\bar{q}q][q1][12][23][3\bar{q}]} . \quad (14)$$

In this formula i and j are the two positive helicity gluons, and i is closer to q than j is in the color ordering. The formula for reversed fermion helicities is

$$A_5^{(\Lambda)}(q^-; 1, 2, 3; \bar{q}^+) = \frac{3i}{\Lambda^2} \frac{[ij]^2 [\bar{q}i]^2 [j\bar{q}][qj]}{[\bar{q}q][q1][12][23][3\bar{q}]}, \quad (15)$$

where now i is the gluon closer to \bar{q} . These amplitudes were constructed to have the correct collinear limits. As a check we calculated $A_5^{(\Lambda)}(q^-; 1^+, 2^+, 3^-; \bar{q}^+)$ from Feynman diagrams.

Notice that the amplitude with reversed quark pair helicities can be obtained by exchanging the quark and anti-quark and reversing the ordering of gluons along the quark line; changing the helicities of the quark-pair amounts to a charge conjugation operation which reverses the color ordering associated with the quark line. Thus equation (15) can be obtained from equation (14).

The required QCD amplitudes are:

$$\begin{aligned} A_5(q^+; 1, 2, 3; \bar{q}^-) &= i \frac{-\langle qi \rangle \langle \bar{q}i \rangle^3}{\langle \bar{q}q \rangle \langle q1 \rangle \langle 12 \rangle \langle 23 \rangle \langle 3\bar{q} \rangle}, \\ A_5(q^-; 1, 2, 3; \bar{q}^+) &= i \frac{\langle \bar{q}i \rangle \langle qi \rangle^3}{\langle \bar{q}q \rangle \langle q1 \rangle \langle 12 \rangle \langle 23 \rangle \langle 3\bar{q} \rangle}, \end{aligned} \quad (16)$$

where i is the negative helicity gluon.

Finally, for the four-quark-one-gluon amplitudes we have,

$$\begin{aligned} A^{(\Lambda)}(q_1^+, \bar{q}_2^-; q_2^+, \bar{q}_1^-; k^+) &= \frac{3i}{\Lambda^2} \frac{[q_1 q_2][q_1 k][q_2 k]}{[\bar{q}_1 q_1][\bar{q}_2 q_2]}, \\ A^{(\Lambda)}(q_1, \bar{q}_1; q_2, \bar{q}_2; k) &= 0. \end{aligned} \quad (17)$$

These amplitudes were inferred from collinear limits, and verified by a Feynman-diagram calculation. Again, amplitudes with reversed quark pair helicities can be obtained by exchanging the quark and anti-quark, and this can be done for each quark-pair separately.

The corresponding QCD amplitudes are:

$$\begin{aligned} \mathcal{A}(q_1^+, \bar{q}_2^-; q_2^+, \bar{q}_1^-; k^+) &= F \frac{\langle q_2 \bar{q}_1 \rangle}{\langle q_2 k \rangle \langle \bar{q}_1 k \rangle}, \\ \mathcal{A}(q_1^+, \bar{q}_1^-; q_2^+, \bar{q}_2^-; k^+) &= F \frac{\langle \bar{q}_2 q_2 \rangle}{\langle q_2 k \rangle \langle \bar{q}_2 k \rangle}, \end{aligned} \quad (18)$$

where

$$F = i \frac{\langle \bar{q}_1 \bar{q}_2 \rangle^2}{\langle \bar{q}_1 q_1 \rangle \langle \bar{q}_2 q_2 \rangle}.$$

Amplitudes with reversed quark-pair helicities can be obtained from (18) by exchanging the appropriate quark and anti-quark in F .

Notice that the expressions in (17), (18) were derived for different quark pair flavors. The amplitudes with same flavor quarks can be obtained from them by antisymmetrizing over identical quarks.

For all the different parton processes, one can obtain the amplitudes with all helicities reversed by parity, which exchanges angle-brackets $\langle \rangle$ and square-brackets $[]$ in (12) – (17), and multiplying by an additional minus sign for amplitudes with an odd number of gluons.

We now need to interfere these amplitudes with the appropriate QCD amplitudes, and to sum over colors and helicities. Since the initial and final states vary from process to process, we perform the initial state averaging later.

For $gg \rightarrow ggg$ we get, summing over final states colors and helicities,

$$\begin{aligned} \delta\sigma_{gggg}^{(\Lambda)} &\equiv \sum_{\text{helicities}} \sum_{\text{colors}} \left(A_5^* A_5^{(\Lambda)} + A_5 A_5^{(\Lambda)*} \right) = \\ &= -6g_s^6 \frac{1}{\Lambda^2} N_c^3 (N_c^2 - 1) \times \\ &\times \left[\sum_{\{2,3,4,5\}} ([1\ 2][2\ 3][3\ 4][4\ 5][5\ 1])^{-2} \sum_{l,m \in \{1,2,\dots,5\}_{l \neq m}} \left([i\ j][j\ k][k\ i][l\ m]^2 \right)^2 + c.c. \right], \end{aligned} \quad (19)$$

where the first summation is over all permutations of (2, 3, 4, 5).

For scattering processes involving four quarks and one gluon, the interference term summed over colors and helicities is,

$$\begin{aligned} \delta\sigma_{q\bar{q}q\bar{q}g}^{(\Lambda)} &= 6g_s^6 \frac{1}{\Lambda^2} N_c (N_c^2 - 1) \frac{1}{\langle \bar{q}_1 q_1 \rangle^2 \langle \bar{q}_2 q_2 \rangle^2} \left(\frac{\langle \bar{q}_1 q_2 \rangle}{\langle \bar{q}_1 k \rangle \langle q_2 k \rangle} - \frac{\langle \bar{q}_2 q_1 \rangle}{\langle \bar{q}_2 k \rangle \langle q_1 k \rangle} \right) \times \\ &\times \left[\langle \bar{q}_1 \bar{q}_2 \rangle^2 \langle q_1 q_2 \rangle \langle q_1 k \rangle \langle q_2 k \rangle + \langle q_1 \bar{q}_2 \rangle^2 \langle \bar{q}_1 q_2 \rangle \langle \bar{q}_1 k \rangle \langle q_2 k \rangle + \right. \\ &\left. + \langle \bar{q}_1 q_2 \rangle^2 \langle q_1 \bar{q}_2 \rangle \langle q_1 k \rangle \langle \bar{q}_2 k \rangle + \langle q_1 q_2 \rangle^2 \langle \bar{q}_1 \bar{q}_2 \rangle \langle \bar{q}_1 k \rangle \langle \bar{q}_2 k \rangle + c.c. \right]. \end{aligned} \quad (20)$$

Again, equation (20) holds for different quark pair flavors, but the modification for same quark flavors is straightforward.

The corresponding expressions for scattering processes involving two quarks and three gluons are more complicated, so we only give here the analytic expression for the color

sum, without summing over helicities. (We perform the latter summation numerically.)

$$\begin{aligned}
\delta\sigma_{q\bar{q}ggg}^{(\Lambda)} &= \frac{(N_c^2 - 1)}{N_c^2} \sum_{\text{helicities}} \left[(N_c^2)^2 \sum_{\{1,2,3\}} A^{(\Lambda)}(1, 2, 3) A^*(1, 2, 3) + \right. \\
&+ N_c^2 \sum_{\{1,2,3\}} A^{(\Lambda)}(1, 2, 3) \left(-2A^*(1, 2, 3) - A^*(2, 1, 3) - A^*(1, 3, 2) + \right. \\
&\left. \left. + A^*(3, 2, 1) \right) + \left(\sum_{\{1,2,3\}} A^{(\Lambda)}(1, 2, 3) \right) \left(\sum_{\{1,2,3\}} A^*(1, 2, 3) \right) + c.c. \right]. \quad (21)
\end{aligned}$$

Here all summations are over the six permutations of $(1, 2, 3)$, and $A(1, 2, 3)$ is shorthand for $A(q; 1, 2, 3; \bar{q})$.

3. Collinear and soft behavior of the $\text{tr}(G^3)$ correction to the cross-section

As is well known, the leading order QCD cross-section for three jet production is singular in the soft and collinear regions of phase-space. This property is exhibited as strong peaking of the QCD distributions near values of the three-jet event variables which correspond to a collinear or to a soft region. In order to search for the $\text{tr}(G^3)$ signal in three jet events it is important to understand its behavior in these regions. As mentioned in the introduction, the special angular dependence of the $\text{tr}(G^3)$ signal in collinear regions can in principle be used to separate it from QCD. In this section we will explain this angular dependence in more detail. First, however, we discuss the behavior of the $\text{tr}(G^3)$ signal in soft regions.

Inspecting the expressions for the interference of QCD amplitudes and $\text{tr}(G^3)$ -induced amplitudes reveals that the different parton energies appear with the same power in the numerator and the denominator in each term, so that the interference remains finite as any of the energies approaches zero. Thus the $\text{tr}(G^3)$ correction to the three jet cross-section remains finite in soft regions of phase-space. Appropriate cuts should therefore be imposed to avoid these regions in searches for $\text{tr}(G^3)$ since the singular QCD background will swamp the signal there.

As for collinear regions, we know that the new amplitudes have collinear singularities since these were used to construct them. For both the QCD and the new amplitudes, the singularity associated with partons i, j becoming collinear is of the form $\langle ij \rangle^{-1}$ or $[ij]^{-1}$, so that its magnitude is $s_{ij}^{-\frac{1}{2}}$. Therefore it results in an s_{ij}^{-1} singularity in the QCD cross-section.

In the following collinear analysis, we hold fixed the helicities of the five external partons, and examine the possible helicities of the effective parton with momentum $k_i + k_j$.

If only one of $\text{Split}_+(i, j)$ and $\text{Split}_-(i, j)$ is non-zero, the resulting singularity in the $\text{tr}(G^3)$ -corrected cross-section is only $s_{ij}^{-\frac{1}{2}}$, because the helicity structures of the four-parton QCD amplitudes and the new amplitudes are orthogonal, so that only one of the two amplitudes in the interference is singular. However, for $gg \rightarrow g$ and $q\bar{q} \rightarrow g$ both $\text{Split}_+(i, j)$ and $\text{Split}_-(i, j)$ can be non-zero, in which case the $\text{tr}(G^3)$ correction to the cross-section has a single pole in s_{ij} . Then, the QCD cross-section and the new cross-section are equally singular in the limit when two partons become collinear. Still, the form of the singularity is different. The singular term in the tree level five-parton QCD cross-section is always of the form $|\text{Split}_\pm(i, j)|^2$ because there is only one choice of the effective parton helicity that yields a non-zero four-parton amplitude, due to the SWI zeroes in equations (9) and (11). In contrast, in the interference of a QCD amplitude with a $\text{tr}(G^3)$ amplitude, the choice of the effective parton helicity is still unique in each amplitude, but it must be of the opposite helicity for the QCD amplitude as for the $\text{tr}(G^3)$ amplitude, due again to four-parton orthogonality. Therefore, the singularity is always of the form $\text{Split}_\pm(i, j)^* \text{Split}_\mp(i, j)$. This last factor carries the phase 2φ , where φ is the angle associated with azimuthal rotations of the two collinear momenta around the direction of their sum, p , with p held fixed. Notice that the phase has to be 2φ rather than φ or it would matter which of the two partons i, j we use to determine φ (exchanging i and j amounts to exchanging φ and $\pi - \varphi$). This is the only φ dependence of the cross-section in the collinear region, as the rest of the expression is just the product of the QCD and $\text{tr}(G^3)$ four-parton amplitudes and they only depend on the four-parton parameters.

As we mentioned above, the trivial φ -dependence of the QCD cross-section follows from the supersymmetric Ward identities. The QCD cross-section has no φ dependence because of the zeroes in equations (9) and (11), and these, in turn, are a consequence of the SWI.

The φ dependence of the cross-section is related to the polarization state of the effective parton. Each QCD five-parton amplitude factorizes on just one four-parton amplitude with either a positive or a negative *circularly*-polarized parton. The resulting QCD cross-section can therefore have no φ dependence. In contrast, each $\text{tr}(G^3)$ -corrected five-parton amplitude factorizes on the sum of two four-parton amplitudes with oppositely polarized gluons. The resulting cross-section contains an interference term corresponding to a *linearly*-polarized effective gluon, and this term gives rise to a non-trivial φ dependence, correlated with the polarization vector.

Since the singular part of the $\text{tr}(G^3)$ correction behaves as $e^{2i\varphi}$ it is washed out upon integrating φ between zero and 2π . The $\text{tr}(G^3)$ correction to the total cross-section is

therefore finite; it has neither soft nor collinear singularities †.

The non-trivial φ dependence of the $\text{tr}(G^3)$ signal can be used to separate it from tree level QCD. If we consider three jet events in a region in which two of the partons are almost-collinear, it is always possible to choose a frame in which the φ dependence of the $\text{tr}(G^3)$ correction is $\cos 2\varphi$. If we then weight the events by $\cos 2\varphi$ and integrate over φ , tree level QCD washes out while the $\text{tr}(G^3)$ contribution remains non-zero. It is useful to define the $\cos 2\varphi$ expectation value,

$$\langle \cos 2\varphi \rangle \equiv \frac{\int \sum (M(M')^* \cos 2\varphi + c.c.)}{\int \sum (M(M')^* + c.c.)}, \quad (22)$$

where M and M' are either the QCD or the $\text{tr}(G^3)$ -induced five-parton amplitudes (depending on whether one is considering the pure QCD signal or the $\text{tr}(G^3)$ correction to the signal), the sum is over colors, helicities and the different relevant parton processes, and the integration is restricted to the almost-collinear region of phase space and sweeps the full range of φ , $0 \leq \varphi \leq 2\pi$. This expectation value is a good probe of the operator $\text{tr}(G^3)$; it receives contributions from the $\text{tr}(G^3)$ correction and no contribution from leading-order QCD. Furthermore, it provides a test of the SWI, or alternatively, of the helicity structure of tree-level QCD.

Notice that four-quark contact operators do not contribute to $\langle \cos 2\varphi \rangle$ at leading-order. These operators only give rise to four-quark one-gluon amplitudes, which can only factorize on four-quark amplitudes containing the four-quark contact vertex, when a quark and a gluon become collinear. Since the helicity of the effective quark is determined by the helicity of the original quark, the same splitting function occurs in both these new amplitudes and the corresponding QCD amplitudes so that the interference has no φ dependence. Thus, these operators do not contribute to the $\cos 2\varphi$ expectation value.

However, some background to the $\text{tr}(G^3)$ signal as measured through this expectation value will arise from higher order QCD effects. A similar azimuthal dependence to the one described above occurs in next-to-leading-order corrections to $2 \rightarrow 3$ scattering and in tree-level $2 \rightarrow 4$ scattering in pure QCD. The first effect turns out to be very small. The collinear behavior of five parton loop amplitudes is similar to equation (6), except there are now two terms [21]. In the first term a “loop splitting-function” multiplies four-point tree amplitudes; here the previous tree-level arguments still forbid an azimuthal dependence.

† This implies that the four-parton loop amplitudes with one insertion of the effective operator, which were mentioned in the introduction, are finite. There are neither ultraviolet nor infrared divergences (soft nor collinear) for them to cancel against. In addition, these loop diagrams have no imaginary parts, as can be seen by cutting them into two tree diagrams and using the orthogonal helicity structures of the QCD and $\text{tr}(G^3)$ four-parton tree diagrams. So they are apt to be quite simple expressions.

In the second term, the usual tree splitting-function multiplies a four-parton QCD loop amplitude; the only azimuthal dependence arises when the loop amplitude is one which vanishes at tree-level. The relative magnitude of this effect compared to the $\text{tr}(G^3)$ signal is given by the relative magnitudes of the $\text{tr}(G^3)$ correction to the four-parton amplitude and the relevant (infrared and ultraviolet finite) four-parton QCD one-loop amplitude. The relevant four-gluon QCD loop amplitude, for example, is [18]

$$A_4^{1\text{-loop}}(1^-, 2^+, 3^+, 4^+) = \frac{i}{48\pi^2} N_c \left(1 - \frac{n_f}{N_c}\right) \frac{\langle 24 \rangle [24]^3}{[12] \langle 23 \rangle \langle 34 \rangle [41]} .$$

Including the coupling constants, it is smaller than the $\text{tr}(G^3)$ amplitude (8) by a factor of the order of $(\Lambda^2/\hat{s})(\alpha_s/18\pi)$. For the values of Λ and \hat{s} relevant for the present analysis (see section 4), this ratio is of the order of $10^{-3} - 10^{-2}$. This estimate is essentially the same as the one mentioned in the introduction where it was remarked that the interference of a QCD loop amplitude with a $\text{tr}(G^3)$ amplitude is small compared with the square of a $\text{tr}(G^3)$ amplitude. A similar estimate holds for quark-gluon amplitudes.

The second source of background, $2 \rightarrow 4$ scattering in pure QCD, is harder to estimate. In this case too there could be a non-trivial dependence on azimuthal rotations of two almost collinear partons, but to get a large correction to the three-jet cross-section one of the remaining two final state partons should be soft or collinear. However, in this limit the six-parton amplitude factorizes on the five-point tree amplitude so there is again a unique possibility for the helicity of the effective parton leading to the conclusion that $2 \rightarrow 4$ QCD contributions to $\langle \cos 2\varphi \rangle$ are probably small.

4. The $\text{tr}(G^3)$ signal in three jet events

We can now proceed to calculate the effect of $\text{tr}(G^3)$ on different distributions in three jet variables. We specifically consider here three jet production at the Tevatron as an example. Since we are only interested in a qualitative estimate of the $\text{tr}(G^3)$ signal, we take the jet momenta to coincide with the parton momenta, without using any hadronization algorithm. We still have to fold the partonic cross-section with the proton, or anti-proton, structure functions:

$$d\sigma = \sum_i \int dx_1 dx_2 F_1(x_1, Q^2) F_2(x_2, Q^2) d\hat{\sigma}_i , \quad (23)$$

where i labels the different partonic processes, and we choose the scale Q as $Q^2 = (x_1 x_2 s)$. We use the DFLM [22] structure functions for the calculation. Here $d\hat{\sigma}_i$ stands for either the QCD cross-section or the $\text{tr}(G^3)$ correction. We evaluate the two simultaneously,

which allows for some checks on the calculation by comparing our results for pure QCD to existing simulations of the QCD distributions (we used the CDF collaboration's results as reported in [23]). Since there is no mass scale in the problem besides Λ (we neglect quark masses), both the QCD cross-section and the $\text{tr}(G^3)$ correction have definite energy scaling properties; the QCD cross-section is energy-independent, and the correction scales as the energy squared. This can be used to factorize the calculation into two parts: an angular integration over final states, and an integration over the incident partons' x_1 and x_2 . This leads to a significant reduction in computer time. We perform the first integral using the Monte-Carlo program SAGE [24].

We also take into account the renormalization of $\text{tr}(G^3)$ between the scales Λ , where $\text{tr}(G^3)$ appears with a coefficient of 4π (see equation (1)), and the scale Q [4]. The anomalous dimension of $\text{tr}(G^3)$ is equal to $\lambda g_s^2/8\pi^2$ with $\lambda = 7 + 2n_f/3$ [25,26] so that the coefficient of $\text{tr}(G^3)$ at the scale Q is,

$$C(Q) = 4\pi \left(\frac{\alpha_s(Q)}{\alpha_s(\Lambda)} \right)^{\frac{\lambda}{2b}}, \quad (24)$$

where $b = -11/2 + n_f/3$ and,

$$\alpha_s(Q) = \frac{\alpha_s(M_z)}{1 - b \frac{\alpha_s(M_z)}{\pi} \log \frac{Q}{M_z}},$$

where we take $\alpha_s(M_z) = 0.118$. The resulting reduction in the coefficient of $\text{tr}(G^3)$ for the relevant values of Λ and Q (see the following) is roughly ten percent. The operator $\text{tr}(G^3)$ does not mix with any other dimension-6 operator through the renormalization group equation [25,26]. In this sense, studying it separately from the other operators is not inconsistent.

We now discuss the geometry of three-jet events (see fig. 1), the cuts we impose and the different distributions we study. We use the notation of the CDF collaboration [23]. Viewed in the center-of-mass system, the three outgoing jets can be described by five independent variables; the total energy of the jets $\sqrt{\hat{s}}$, and four scale-independent quantities, namely, the energy fractions of two of the jets, and two angles. Labeling the jets 3, 4 and 5, in order of decreasing energies, the energy fraction of jet i is defined as

$$x_i = \frac{2E_i}{\sqrt{\hat{s}}}, \quad i = 3, 4, 5, \quad (25)$$

where E_i is the energy of the i -th jet, and $x_3 + x_4 + x_5 = 2$. The angles we use are the angle between the fastest jet and the beam direction, θ , and the angle between the jets'

plane and the plane of the fastest jet and the beam, ψ . An additional angle, the overall azimuthal angle around the beam direction, is required for a full description of the event, but the dependence on it is trivial for unpolarized beams.

We describe here three different ways of probing $\text{tr}(G^3)$. The first is to study distributions in various three jet variables in the region where the three jets are hard and well separated. The second is to study the $\cos 2\varphi$ expectation value of equation (22) obtained by weighting the relevant matrix elements by $\cos 2\varphi$ in the region where jets 4 and 5 are almost collinear as discussed in section 3. Finally, one can interpolate between these two regions and study distributions which reflect the qualitative differences between the QCD cross-section and the $\text{tr}(G^3)$ correction in the cross-over region.

To ensure that the three jets are well separated we impose the following set of cuts (set A)

$$\begin{aligned}
\sqrt{\hat{s}} &\geq 250 \text{ GeV} , \\
x_3 &\leq 0.8 , \\
|\cos \theta| &\leq 0.8 , \\
30^\circ &\leq \psi \leq 150^\circ .
\end{aligned}
\tag{26}$$

We take the lower bound on the total jet energy, $\sqrt{\hat{s}}$, to be 250 GeV for the Tevatron following ref. [23]. Increasing this bound enhances the deviation from QCD, but decreases the cross-section, thus leading to poorer statistics. The energy fraction of the fastest jet, x_3 , varies between $\frac{2}{3}$ and 1. The former value corresponds to a symmetric event, and the latter to either a soft jet (5) or to two collinear jets (4 and 5). It is therefore necessary to set some cut on the maximum value of x_3 to avoid soft or collinear jets. As this cut decreases, the sensitivity of the signal to the deviation from QCD improves, since it drives the events away from the soft region, where QCD is divergent whereas the deviation is finite. We take the x_3 cut to be 0.8. To avoid regions where jet 3 becomes collinear with the beam direction, we require that the absolute value of $\cos \theta$ be smaller than 0.8. Finally, to prevent jets 4 and 5 from approaching the beam direction we take ψ to lie between 30° and 150° .

The distributions in x_3 , ψ and the three jet invariant mass $\sqrt{\hat{s}}$ for the scale $\Lambda = 1$ TeV are plotted in Fig. 2. The errors bars shown are the estimated statistical errors assuming an integrated luminosity of 15pb^{-1} . The $\text{tr}(G^3)$ correction to all three distributions is positive throughout this range. The deviations from QCD change sign because we plot normalized distributions following the CDF conventions. Even though the shape of the $\text{tr}(G^3)$ correction is different from the shape of the QCD distributions for these variables, when added to the larger QCD cross-sections they still result in distributions that are

qualitatively similar to the QCD distributions, apart, roughly, from a vertical shift. Thus, the effect of $\text{tr}(G^3)$ on the normalized distributions is quite small in this region, and although it is larger than the estimated statistical errors, it seems unlikely that studying this region by itself could conclusively determine the presence of the effective operator.

We have also computed distributions in $\cos^{-1}((x_4 - x_5)/x_3)$, as suggested by Ellis, Karliner and Stirling [10], in $(1 + \cos \theta)/(1 - \cos \theta)$, following ref. [9] and in x_4 and θ . None of them improves the sensitivity to the signal.

The situation becomes even worse if one includes a form-factor in the analysis. The operator $\text{tr}(G^3)$ violates unitarity in $2 \rightarrow 2$ parton scattering as discussed by Dreiner *et al.* [6]. These authors replace $1/\Lambda^2$ by

$$\frac{1}{\Lambda^2} \frac{1}{(1 + 4\pi\hat{s}/(3\Lambda^2))^2} \quad (27)$$

where \hat{s} is the parton center-of-mass energy, to restore unitarity in most partial waves in the $2 \rightarrow 2$ scattering †. Since the $\text{tr}(G^3)$ signal in dijet production is $O(\hat{s}^2/\Lambda^4)$ it is greatly reduced by the form-factor. In the case at hand, the effect of the form-factor is smaller but it still reduces the already-small $\text{tr}(G^3)$ signal of Fig. 2.

Alternatively, the effective operator can be probed in the second way mentioned above, namely, by focusing on the collinear region and using the φ dependence of the correction induced by the effective operator to detect it. To get to the region where jets 4 and 5 are almost collinear and neither is soft we take $x_3 \geq 0.95$ and $x_5 \geq 0.3$. We need some further cut to ensure that the two jets are still distinguishable. If we were to use a standard jet algorithm which involves $R = \sqrt{(\Delta\eta)^2 + (\Delta\phi)^2}$, where η is the jet's rapidity and ϕ is the usual azimuthal angle of the jet, in order to achieve this, we would introduce a spurious φ -dependence which would spoil the effect we describe here. Instead it would probably be best to impose a cut on the minimum transverse momentum of jets 4 and 5 with respect to the direction of jet 3 ‡ (this direction is the direction of the boost to the rest frame of jets 4 and 5). However, since we factorize the calculation into independent integrations over x_1, x_2 and over the final states, we impose the stricter cut:

$$x_4 \sin \theta_{34} \geq \frac{5\text{GeV}}{(\sqrt{\hat{s}})_{min}/2}, \quad (28)$$

where θ_{34} is the angle between jets 3 and 4. Combined with the cut on \hat{s} , $\hat{s} \geq \hat{s}_{min}$, this cut guarantees that the transverse momentum of jets 4 and 5 is greater than 5 GeV.

† Here we modified the numerical factor to take into account the different scale definitions. The scale Λ used by Dreiner *et al.* is equal to our $\Lambda/\sqrt{16\pi}$.

‡ We thank J. D. Bjorken for suggesting this.

In addition, we take $|\cos\theta| \leq 0.5$ so that the 2-jet-like event is almost perpendicular to the beam direction and the $\text{tr}(G^3)$ correction is more pronounced. However, we impose no cuts on the angle ψ . This angle should be allowed to sweep its entire range so that the azimuthal angle φ of jets 4 and 5 can vary between zero and 2π .

We collect these cuts (set B) here

$$\begin{aligned}
\sqrt{\hat{s}} &\geq 250 \text{ GeV} , \\
x_3 &\geq 0.95 , \\
x_5 &\geq 0.3 , \\
x_4 \sin\theta_{34} &\geq \frac{5\text{GeV}}{(\sqrt{\hat{s}})_{\min}/2} , \\
|\cos\theta| &\leq 0.5 .
\end{aligned} \tag{29}$$

The resulting QCD and $\text{tr}(G^3)$ -corrected distributions in x_3 and in the cosine of the angle between jets 4 and 5, $\cos\theta_{45}$, are plotted in Fig. 3. Again, the error bars shown are the estimated statistical errors assuming an integrated luminosity of 15pb^{-1} . In 3a and 3b we plot the distributions obtained by weighting the matrix elements with $\cos 2\varphi$,

$$\frac{d\sigma_\varphi}{d\cos\theta_{45}} = \int d\varphi \cos 2\varphi \frac{d^2\sigma}{d\varphi d\cos\theta_{45}} = \langle \cos 2\varphi \rangle \frac{d\sigma}{d\cos\theta_{45}} , \tag{30}$$

and,

$$\frac{d\sigma_\varphi}{dx_3} = \int d\varphi \cos 2\varphi \frac{d^2\sigma}{d\varphi dx_3} = \langle \cos 2\varphi \rangle \frac{d\sigma}{dx_3} , \tag{31}$$

where $\langle \cos 2\varphi \rangle$ of (30) is different than that of (31) as they are distributed in different variables. In this case the angle φ is the azimuthal angle of jet 4 around the sum of the momenta of jets 4 and 5, and it is related to the angle ψ : $\varphi = \psi - \pi/2$. The resulting distributions are negative as they receive larger contributions from events that are co-planar with the beam. The magnitude of the QCD distributions decreases on approaching the collinear limit while the magnitude of the $\text{tr}(G^3)$ correction grows. In 3c and 3d we show $\langle \cos 2\varphi \rangle$ as obtained from QCD with and without $\text{tr}(G^3)$. Clearly, the signal is dominated by the $\text{tr}(G^3)$ correction. Also shown are the $\text{tr}(G^3)$ -corrected distributions with the form-factor (27) included. The form-factor reduces the $\text{tr}(G^3)$ correction uniformly over the entire x_3 and $\cos\theta_{45}$ ranges. The reduction factor is equal to the scale-averaged form-factor, and is about one half, which is roughly the value of the form-factor near the cut $\sqrt{\hat{s}} = 250 \text{ GeV}$, from where most of the cross-section comes.

Recall that the $\text{tr}(G^3)$ correction to the cross-section has a non-trivial φ -dependence only if the collinear partons are a quark and an anti-quark or two gluons with opposite

helicities. Therefore if quark and gluon jets could be separated experimentally (a difficult task) one could get a larger $\langle \cos 2\varphi \rangle$ signal by only considering collinear gluon pairs or quark anti-quark pairs.

This method provides a distinctive probe of $\text{tr}(G^3)$. The $\cos 2\varphi$ expectation value is dominated by the $\text{tr}(G^3)$ correction and does not receive contributions from the tree-level five-parton QCD cross-section or from dimension-6 operators that can be related to four-quark contact operators. One source of background to this measurement is higher-order contributions to the QCD cross-section which have a non-trivial dependence on azimuthal rotations in the collinear region. As discussed earlier, these contributions are probably quite small. Some azimuthal dependence could also arise from color-strings associated with the hadronization of the out-going partons. The magnitude of these effects can be estimated by combining the exact five-parton cross-section with Monte-Carlo simulations for parton showers and hadronization, but we have not done so here. Also, the different dependence of the effective operator contribution on the parton center-of-mass energy could be used to separate its signal from these QCD backgrounds. In addition to these theoretical issues, there are experimental difficulties associated with measuring the azimuthal dependence of almost collinear jets. In particular, both the algorithm used to define these jets and the detector should not induce a significant spurious azimuthal dependence; the $\cos 2\varphi$ asymmetry is only a few percent for the value of Λ considered here.

So far we have considered the effects of $\text{tr}(G^3)$ in two regions: one where the three jets are well separated, and the other where two jets are almost collinear. The $\text{tr}(G^3)$ correction is positive in the first region and negative in the second. (The sign of the effect is reversed if the coefficient of the operator is negative.) One can use this fact to enhance the $\text{tr}(G^3)$ signal by studying *normalized* distributions in a variable which parametrizes the extent of collinearity, such as the angle between jets 4 and 5 or x_3 , over a wide region which includes both the region where the jets are well separated and the region where they become collinear. Since the $\text{tr}(G^3)$ corrections change sign over this region the resulting normalized distributions are more sensitive to the $\text{tr}(G^3)$ signal compared to studies which avoid the collinear region altogether. This is indeed the case as one can see in Fig. 4 where we plot the normalized distributions in x_3 with x_3 varying from its minimum value, $2/3$, all the way up to 0.95. Here we combine the cuts on $\cos\theta$ and on ψ of set A (26) which ensure that the five partons are well separated outside the collinear region, with the cuts on x_5 and on the p_T of jets 4 and 5 of set B (29) so that jets 4 and 5 are still distinguishable

when the collinear region is approached. We label these cuts as set C,

$$\begin{aligned}
\sqrt{\hat{s}} &\geq 250 \text{ GeV} , \\
x_3 &\leq 0.95 , \\
x_5 &\geq 0.3 , \\
x_4 \sin \theta_{34} &\geq \frac{5\text{GeV}}{(\sqrt{\hat{s}})_{\min}/2} , \\
|\cos \theta| &\leq 0.8 , \\
30^\circ &\leq \psi \leq 150^\circ .
\end{aligned} \tag{32}$$

The deviation due to $\text{tr}(G^3)$ is more pronounced here than in Fig. 2, where the x_3 distribution is evaluated in the region where the jets are well separated. Again, the errors bars shown are the estimated statistical errors assuming an integrated luminosity of 15 pb^{-1} . Except in the cross-over region where it changes sign, the deviation from QCD is significantly larger than these errors. For x_3 between 0.7 and 0.8 the deviation from QCD is about twenty-five percent of the QCD result.

To exhibit the energy dependence of the $\text{tr}(G^3)$ signal we also study the difference between the cross-section above the cross-over point, which is roughly $x_3 = .88$, and the cross-section below this point, with and without the $\text{tr}(G^3)$ correction. This quantity is sensitive to the $\text{tr}(G^3)$ signal because the $\text{tr}(G^3)$ correction changes sign near $x_3 = .88$. In Fig. 5 we show the difference between the sum of the last three bins in the x_3 distributions of Fig. 4 (bins 10, 11 and 12) and the sum of the three bins below them (bins 7, 8 and 9) divided by the sum of all six bins for different values of $\sqrt{\hat{s}}$,

$$r_{0.88} = \frac{\left(\frac{d\sigma}{d\sqrt{\hat{s}}}\right)_{.88 \leq x_3 \leq .95} - \left(\frac{d\sigma}{d\sqrt{\hat{s}}}\right)_{.81 \leq x_3 \leq .88}}{\left(\frac{d\sigma}{d\sqrt{\hat{s}}}\right)_{.88 \leq x_3 \leq .95} + \left(\frac{d\sigma}{d\sqrt{\hat{s}}}\right)_{.81 \leq x_3 \leq .88}} \tag{33}$$

The deviations from QCD are very large in this case, and the different energy dependence of the two signals is clearly seen. However, including the form-factor (27) flattens the $\text{tr}(G^3)$ correction and reduces the deviation from QCD to the point where it is smaller than, or on the order of the statistical errors.

We have discussed three approaches to probing $\text{tr}(G^3)$: one which is limited to the region where the three jets are well separated, one which focuses on the collinear region and one which combines these two regions. The last two are more sensitive to the $\text{tr}(G^3)$ signal. All the distributions we study are normalized distributions. This should reduce some of the systematic errors in performing the measurements.

In most of our analysis we have included the effects of a form-factor on the deviations from QCD due to the operator $\text{tr}(G^3)$. This is not usually done in similar searches for quark substructure. Studying the effects of a form-factor on the $\text{tr}(G^3)$ signal became necessary in the context of dijet production, where this operator only contributes at order $O(1/\Lambda^4)$ so that the parametrization in terms of the effective operator breaks down at energies where the signal becomes appreciable. In that case the form-factor greatly reduces the $\text{tr}(G^3)$ signal [6]. In the case at hand the effect of the form-factor is smaller, but non-negligible. Furthermore, unlike similar searches for quark substructure which use the p_T or some other energy-dependent distributions, and are therefore sensitive to the effects of form-factors, most of the distributions we consider here are distributions in energy-independent quantities such as angles and energy fractions. A form-factor therefore only reduces the deviation from QCD uniformly over the entire range, by a factor which is equal to the energy averaged value of the form-factor, without changing the qualitative shape of the distributions.

Throughout this discussion, we took the cut on the minimum center-of-mass energy of the jets, $\sqrt{\hat{s}}$, to be rather low – 250 GeV, as used in early CDF studies [23] of three-jet events. With the larger integrated luminosity now available at the Tevatron, this cut can be increased in order to enhance the $\text{tr}(G^3)$ signal. Varying this cut also allows one to distinguish between the $\text{tr}(G^3)$ signal and higher order QCD effects which have different power-law dependences on the parton center-of-mass energy $\sqrt{\hat{s}}$.

Finally, a remark regarding the choice of μ of the coupling constant $\alpha_s(\mu)$ is in order. In regions where the three jets are well defined the results are not very sensitive to this choice but it becomes relevant in regions where two of the jets approach collinearity. The $\cos 2\varphi$ expectation value in this region is obtained by normalizing the $\cos 2\varphi$ weighted distributions by the non-weighted distributions so it is insensitive to the value of the coupling. However, the x_3 distribution which interpolates between the collinear and the non-collinear regions would probably be affected. Since in this paper we only present qualitative tree-level results this effect was not taken into account.

5. Conclusions

As discussed in section 1, the operator $\text{tr}(G^3)$ cannot be reliably probed through dijet production or inclusive jet production in hadron colliders. Jet production in e^+e^- machines cannot yield good bounds on the scale Λ because of the low characteristic center-of-mass energy. This leaves three jet production in hadron colliders as the best place to probe the gluonic operator $\text{tr}(G^3)$. In this case $\text{tr}(G^3)$ contributes at leading order in $1/\Lambda^2$.

We have suggested two complementary ways of detecting the $\text{tr}(G^3)$ signal. One involves studying the region where two of the jets are almost collinear, and the other interpolates between the collinear region and the region where the three jets are well separated. These approaches appear to have better analyzing power than tests that avoid the collinear region altogether, since the deviations from QCD are more pronounced in the collinear region. The two approaches may still be rather challenging experimentally.

In the collinear region the $\text{tr}(G^3)$ correction, unlike the tree-level QCD cross-section, has a non-trivial behavior under azimuthal rotations of the collinear momenta that leave their sum unchanged. Weighting the cross-section by the appropriate function of this azimuthal angle can in principle allow us to separate the $\text{tr}(G^3)$ signal from QCD. The fact that the tree-level QCD cross-section is invariant under these azimuthal rotations follows from the helicity structure of the four-parton QCD amplitudes at tree-level, which in turn follows from the supersymmetric Ward identities. Thus, measuring the dependence of the collinear three-jet cross-section on this azimuthal angle provides a test of the helicity structure of tree-level QCD and the SWI, as well as a method for probing new physics in the strong-interaction sector via the effective operator $\text{tr}(G^3)$.

Acknowledgements

We thank L. Randall for her collaboration at an early stage of this work. We also thank J. D. Bjorken and D. Zeppenfeld for useful discussions, Z. Bern for loop polynomial assistance, and H. Haber for help with the SAGE program. Finally, it is a pleasure to thank M. Peskin for reading the manuscript and for insightful suggestions.

Appendix: Collinear properties of color-ordered sub-amplitudes

In this appendix we discuss additional details of color ordered sub-amplitudes, the helicity basis and collinear factorization. Except for the behavior of the $\text{tr}(G^3)$ three-gluon vertex in the collinear limits, all the results mentioned are well known (see the review paper by Mangano and Parke [16] and references therein) and are summarized here for the reader's convenience.

The gluon sub-amplitudes (2) have the following properties:

- $A_n(1, 2, \dots, n)$ is invariant under cyclic permutations.
- $A_n(n, n-1, \dots, 1) = (-1)^n A_n(1, 2, \dots, n)$
- $A_n(1, 2, 3, \dots, n) + A_n(2, 1, 3, \dots, n) + \dots + A_n(2, 3, \dots, 1, n) = 0$

The last equation is due to the decoupling of the $U(1)$ gauge boson in a $U(N)$ gauge theory. These relations reduce the number of independent sub-amplitudes that have to be calculated.

We now turn to discuss collinear factorization in the color-ordered basis. Equation (6) of section 2 can be proven from the string representation of gauge theory tree amplitudes [16] but here we will briefly discuss it from the point of view of Feynman diagrams. In the limit when partons i and j become collinear, the n -parton color ordered sub-amplitude with $n \geq 5$ can become singular as the relevant propagator goes on-shell. This only happens if the collinear partons are color-adjacent; they have to be attached to the same three-parton vertex to give rise to an on-shell propagator. The singularity may be removed by powers of the Lorentz invariant s_{ij} coming from the vertex. However, for most helicity choices of i and j and λ , the QCD three-parton vertex contracted with the polarization vectors of i and j (or spinors, for quarks), behaves as $\sqrt{s_{ij}}$ at leading order so that the singularity remains, although it is reduced to $1/\sqrt{s_{ij}}$. Furthermore, the coefficient of the $\sqrt{s_{ij}}$ term in the vertex can be replaced, up to a numerical factor, by the polarization vector of an effective external parton with momentum $p = k_i + k_j$ and helicity λ . The remaining part of the diagram, contracted with the effective parton, becomes an $(n - 1)$ -parton diagram, and summing over all possible diagrams gives the $(n - 1)$ -parton amplitude, multiplied by the splitting function.

We now show that no additional collinear singularities arise from the gluon operator $\text{tr}(G^3)$. The only issue is for the quark-free $g \rightarrow gg$ singularity. Contracting the new three gluon vertex with the polarization vectors ε_1 and ε_2 of the external gluons 1 and 2 and using momentum conservation and the gluons' transversality, $\varepsilon_1 \cdot k_1 = \varepsilon_2 \cdot k_2 = 0$, this vertex can be simplified to the form

$$(k_1 \cdot \varepsilon_2 k_2 \cdot \varepsilon_1 - k_1 \cdot k_2 \varepsilon_1 \cdot \varepsilon_2) (k_2 - k_1)^\mu, \quad (34)$$

up to an overall factor which does not depend on the momenta k_1, k_2 of the gluons[†].

In the limit where k_1 and k_2 become collinear, we can write $k_1 = zp + q$, $k_2 = (1 - z)p - q$, where z is a number and $q^\mu \rightarrow 0$. Eliminating p from these relations we can express k_1 as a combination of q and k_2 and vice versa. Using $\varepsilon_1 \cdot k_1 = \varepsilon_2 \cdot k_2 = 0$ the first term in eqn. (34) becomes

$$k_1 \cdot \varepsilon_2 k_2 \cdot \varepsilon_1 \propto q \cdot \varepsilon_2 q \cdot \varepsilon_1.$$

But since the on-shell propagator is $1/(k_1 + k_2)^2$ and

$$(k_1 + k_2)^2 = 2k_1 \cdot k_2 = p^2 = O(q^2) = O(p \cdot q),$$

[†] If the two gluons have opposite helicities, one can choose the reference momentum of 1 to be k_2 and vice versa so that the vertex vanishes for arbitrary k_1 and k_2 .

we see that both terms in the vertex go to zero at least as fast as $(k_1 + k_2)^2$ so that the singularity cancels.

The explicit representation of the spinor products that we use follows ref. [16]. For two momenta with positive energies:

$$\langle ij \rangle \equiv \sqrt{s_{ij}} \exp(i\phi_{ij}), \quad (35)$$

where $s_{ij} = 2p_i \cdot p_j$, and

$$\cos \phi_{ij} = (p_i^1 p_j^+ - p_j^1 p_i^+) / \sqrt{p_i^+ p_j^+ s_{ij}}, \quad \sin \phi_{ij} = (p_i^2 p_j^+ - p_j^2 p_i^+) / \sqrt{p_i^+ p_j^+ s_{ij}},$$

where $p^\pm = (p^0 \pm p^3)$. If any of the momenta has negative energy, the spinor product is calculated with minus that momentum and then multiplied by i for each negative energy momentum. $[ij]$ can be calculated using $\langle ij \rangle [ji] = s_{ij}$ and the antisymmetry of the spinor products, $\langle ij \rangle = -\langle ji \rangle$, $[ij] = -[ji]$.

We collect here the tree-level splitting-functions used to infer the $\text{tr}(G^3)$ correction to five-parton amplitudes.

The $g \rightarrow gg$ splitting functions are

$$\begin{aligned} \text{Split}_+(i^+, j^+) &= 0, \\ \text{Split}_-(i^-, j^-) &= 0, \\ \text{Split}_-(i^+, j^+) &= \frac{1}{\sqrt{z(1-z)} \langle ij \rangle}, \\ \text{Split}_+(i^-, j^-) &= -\frac{1}{\sqrt{z(1-z)} [ij]}, \\ \text{Split}_-(i^+, j^-) &= -\frac{z^2}{\sqrt{z(1-z)} [ij]}, \\ \text{Split}_+(i^+, j^-) &= \frac{(1-z)^2}{\sqrt{z(1-z)} \langle ij \rangle}, \\ \text{Split}_+(i^-, j^+) &= \frac{z^2}{\sqrt{z(1-z)} \langle ij \rangle}, \\ \text{Split}_-(i^-, j^+) &= -\frac{(1-z)^2}{\sqrt{z(1-z)} [ij]}, \end{aligned} \quad (36)$$

the $g \rightarrow \bar{q}q$ splitting functions are

$$\begin{aligned}
\text{Split}_+(\bar{q}^+, q^-) &= \frac{z^{1/2}(1-z)^{3/2}}{\sqrt{z(1-z)} \langle \bar{q} q \rangle}, \\
\text{Split}_+(\bar{q}^-, q^+) &= -\frac{z^{3/2}(1-z)^{1/2}}{\sqrt{z(1-z)} \langle \bar{q} q \rangle}, \\
\text{Split}_-(\bar{q}^+, q^-) &= \frac{z^{3/2}(1-z)^{1/2}}{\sqrt{z(1-z)} [\bar{q} q]}, \\
\text{Split}_-(\bar{q}^-, q^+) &= -\frac{z^{1/2}(1-z)^{3/2}}{\sqrt{z(1-z)} [\bar{q} q]},
\end{aligned} \tag{37}$$

and the $q \rightarrow qg$ and $\bar{q} \rightarrow g\bar{q}$ splitting functions are

$$\begin{aligned}
\text{Split}_+(q^-, i^+) &= \frac{z^{3/2}}{\sqrt{z(1-z)} \langle q i \rangle}, \\
\text{Split}_+(q^-, i^-) &= -\frac{z^{1/2}}{\sqrt{z(1-z)} [q i]}, \\
\text{Split}_-(q^+, i^+) &= \frac{z^{1/2}}{\sqrt{z(1-z)} \langle q i \rangle}, \\
\text{Split}_-(q^+, i^-) &= -\frac{z^{3/2}}{\sqrt{z(1-z)} [q i]}, \\
\text{Split}_-(i^+, \bar{q}^+) &= \frac{(1-z)^{1/2}}{\sqrt{z(1-z)} \langle i \bar{q} \rangle}, \\
\text{Split}_-(i^-, \bar{q}^+) &= -\frac{(1-z)^{3/2}}{\sqrt{z(1-z)} [i \bar{q}]}, \\
\text{Split}_+(i^+, \bar{q}^-) &= \frac{(1-z)^{3/2}}{\sqrt{z(1-z)} \langle i \bar{q} \rangle}, \\
\text{Split}_+(i^-, \bar{q}^-) &= -\frac{(1-z)^{1/2}}{\sqrt{z(1-z)} [i \bar{q}]}.
\end{aligned} \tag{38}$$

Here z denotes the collinear momentum fraction, so that $k_i = zp$, $k_j = (1-z)p$, with p denoting the sum of the collinear momenta. Note that reversing all helicities (parity) is equivalent to exchanging $\langle \rangle$ and $[\]$, and inserting a minus sign.

References

- [1] E. Eichten, K. Lane, and M. Peskin, Phys. Rev. Lett. 50 (1983) 811.
- [2] CDF Collaboration, F. Abe *et al.*, FERMILAB-PUB-93/151-E.
- [3] E.H. Simmons, Phys. Lett. B226 (1989) 132; Phys. Lett. B246 (1990) 471.
- [4] P. Cho and E. Simmons, preprint HUTP-93/A018, hep-ph/9307345.
- [5] A. Duff and D. Zeppenfeld, Z. Phys. C53 (1992) 529.
- [6] H. Dreiner, A. Duff and D. Zeppenfeld, Phys. Lett. B282 (1992) 441.
- [7] Z. Bern and D. A. Kosower, Phys. Rev. Lett. 66 (1991) 1669; Nucl. Phys. B379 (1992) 451.
- [8] Z. Kunszt, A. Signer and Z. Trocsanyi, preprint ETH-TH/93-11, hep-ph/9305239.
- [9] E. Argyres, G. Katsilieris, C. Papadopoulos, and S. Vlassopoulos, Int. J. Mod. Phys. A7 (1992) 7915.
- [10] J. Ellis, I. Karliner and W. Stirling, Phys. Lett. B217 (1989) 363.
- [11] M.T. Grisaru, H.N. Pendleton and P. van Nieuwenhuizen, Phys. Rev. D15 (1977) 996; M.T. Grisaru and H.N. Pendleton, Nucl. Phys. B124 (1977) 81.
- [12] M. Mangano and S.J. Parke, Nucl. Phys. B299 (1988) 653.
- [13] S. Parke and T. Taylor, Phys. Lett. B157 (1985) 81.
- [14] F. A. Berends and W. T. Giele, Nucl. Phys. B294 (1987) 700; M. Mangano, S. J. Parke and Z. Xu, Nucl. Phys. B298 (1988) 653; M. Mangano, S. J. Parke, Nucl. Phys. B299 (1988) 673; D. Zeppenfeld, Int. J. Mod. Phys. A3 (1988) 2175.
- [15] F. A. Berends, R. Kleiss, P. De Causmaecker, R. Gastmans, and T. T. Wu, Phys. Lett. B103 (1981) 124; P. De Causmaecker, R. Gastmans, W. Troost, and T. T. Wu, Nucl. Phys. B206 (1982) 53. R. Kleiss and W. J. Stirling, Nucl. Phys. B262 (1985) 235; J. F. Gunion and Z. Kunszt, Phys. Lett. B161 (1985) 333; R. Gastmans and T.T. Wu, *The Ubiquitous Photon: Helicity Method for QED and QCD* (Clarendon Press) (1990).
- [16] M. Mangano and S. J. Parke, Phys. Rept. 200 (1991) 301.
- [17] F. A. Berends and W. T. Giele, Nucl. Phys. B306 (1988) 759.
- [18] Z. Bern, L. Dixon and D. Kosower, Phys. Rev. Lett. 70 (1993) 2677.
- [19] G. Altarelli and G. Parisi, Nucl. Phys. B126 (1977) 298.
- [20] Z. Bern, G. Chalmers, L. Dixon and D. A. Kosower, preprint SLAC-PUB-6409, hep-ph/9312333.
- [21] Z. Bern, L. Dixon, D. Dunbar and D. A. Kosower, in preparation.

- [22] M. Diemoz, F. Ferroni, E. Longo and G. Martinelli, Z. Phys. C39 (1988) 21 (set 1).
- [23] CDF collaboration, F. Abe *et al.*, Phys. Rev. D45 (1992) 1448.
- [24] J. H. Friedman, J. Comp. Physics, 7 (1971) 1.
- [25] A. Y. Morozov, Sov. J. Nucl. Phys. 40 (1984) 505.
- [26] S. Narison and R. Tarrach, Phys. Lett. B125 (1983) 217.

Figure Captions:

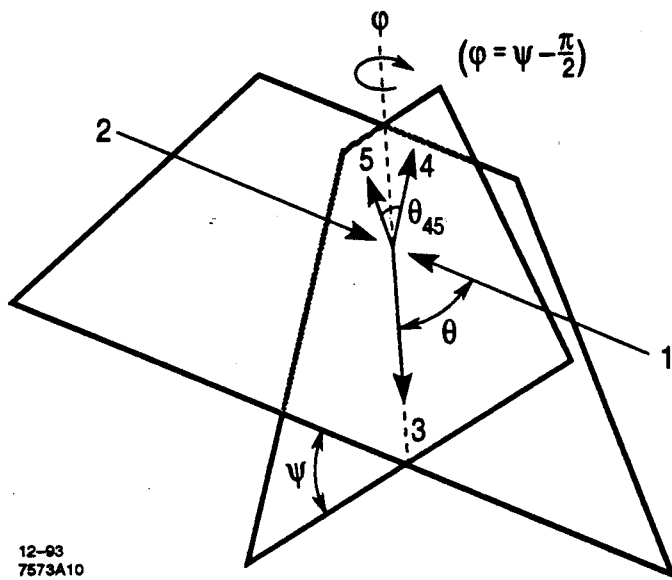
Figure 1: The three jet event in the parton center-of-mass frame. The parton momenta are not drawn to scale.

Figure 2: Effect of $\text{tr}(G^3)$ on various distributions in three jet event variables at $\sqrt{s} = 1.8$ TeV in the region where the jets are well separated. The solid line gives the QCD prediction, and the dashed line includes the $\text{tr}(G^3)$ correction with $\Lambda = 1$ TeV, with the cuts of set A (equation (26)). The error bars are the estimated statistical errors for an integrated luminosity of 15 pb^{-1} .

Figure 3: Effect of $\text{tr}(G^3)$ on various distributions of three jet event variables at $\sqrt{s} = 1.8$ TeV in the region where two of the jets are almost collinear. The solid line gives the QCD prediction, the other two lines include the $\text{tr}(G^3)$ correction with $\Lambda = 1$ TeV without (dashes) and with (dot-dashes) the form-factor $(1 + 4\pi\hat{s}/(3\Lambda^2))^{-2}$. Here we impose the cuts of set B (equation (29)). The error bars are the estimated statistical errors for an integrated luminosity of 15 pb^{-1} .

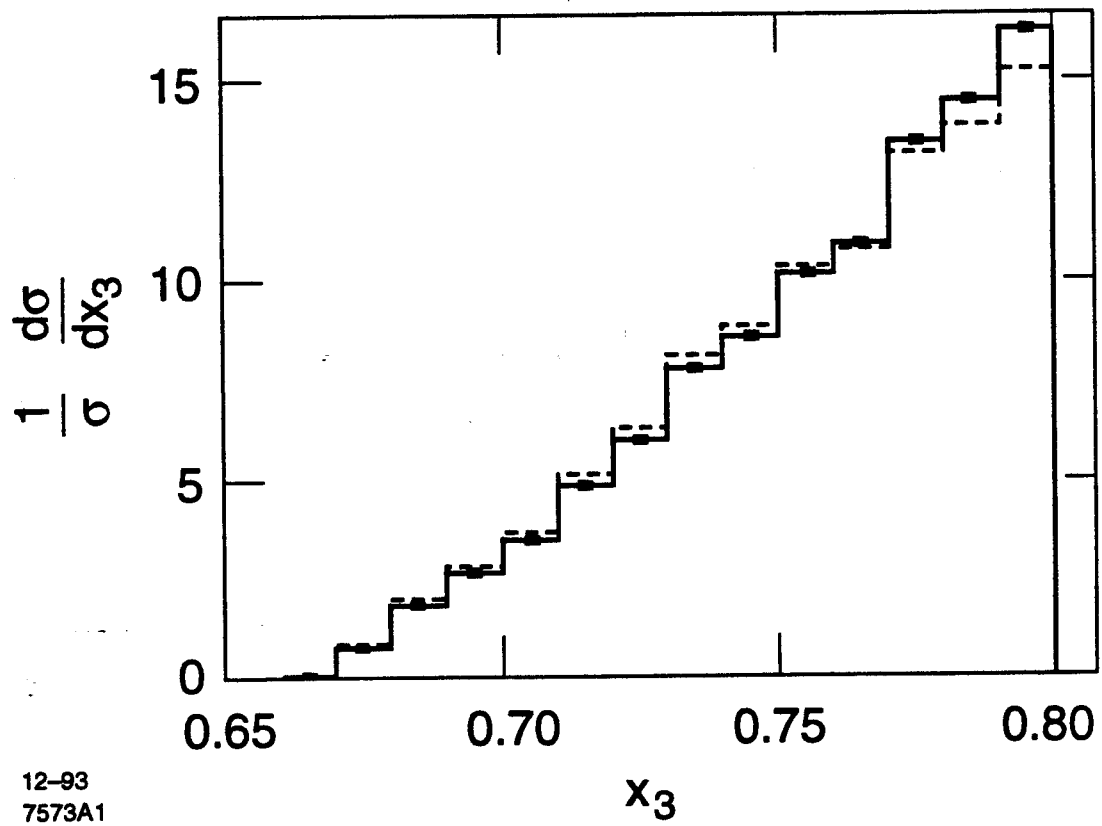
Figure 4: Effect of $\text{tr}(G^3)$ on the x_3 distribution at $\sqrt{s} = 1.8$ TeV in the cross-over region. The solid line gives the QCD prediction, the other two lines include the $\text{tr}(G^3)$ correction with $\Lambda = 1$ TeV without (dashes) and with (dot-dashes) the form-factor $(1 + 4\pi\hat{s}/(3\Lambda^2))^{-2}$. Here we impose the cuts of set C (equation (32)). The error bars are the estimated statistical errors for an integrated luminosity of 15 pb^{-1} .

Figure 5: The difference between the last three (10,11,12) bins and the three bins below them (7,8,9) of the x_3 distribution of Fig. 3, divided by the sum of the bins, as a function of $\sqrt{\hat{s}}$. The error bars are the estimated statistical errors for an integrated luminosity of 15 pb^{-1} .



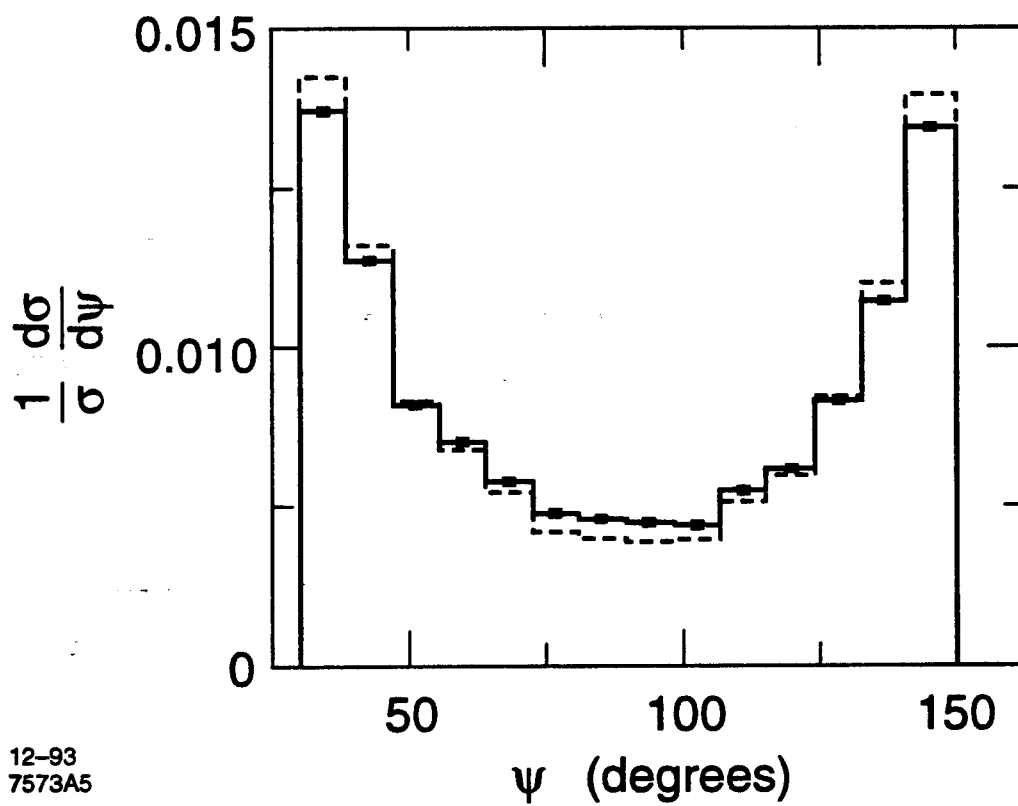
12-93
7573A10

Fig. 1



12-93
7573A1

Fig. 2a



12-93
7573A5

Fig. 2b

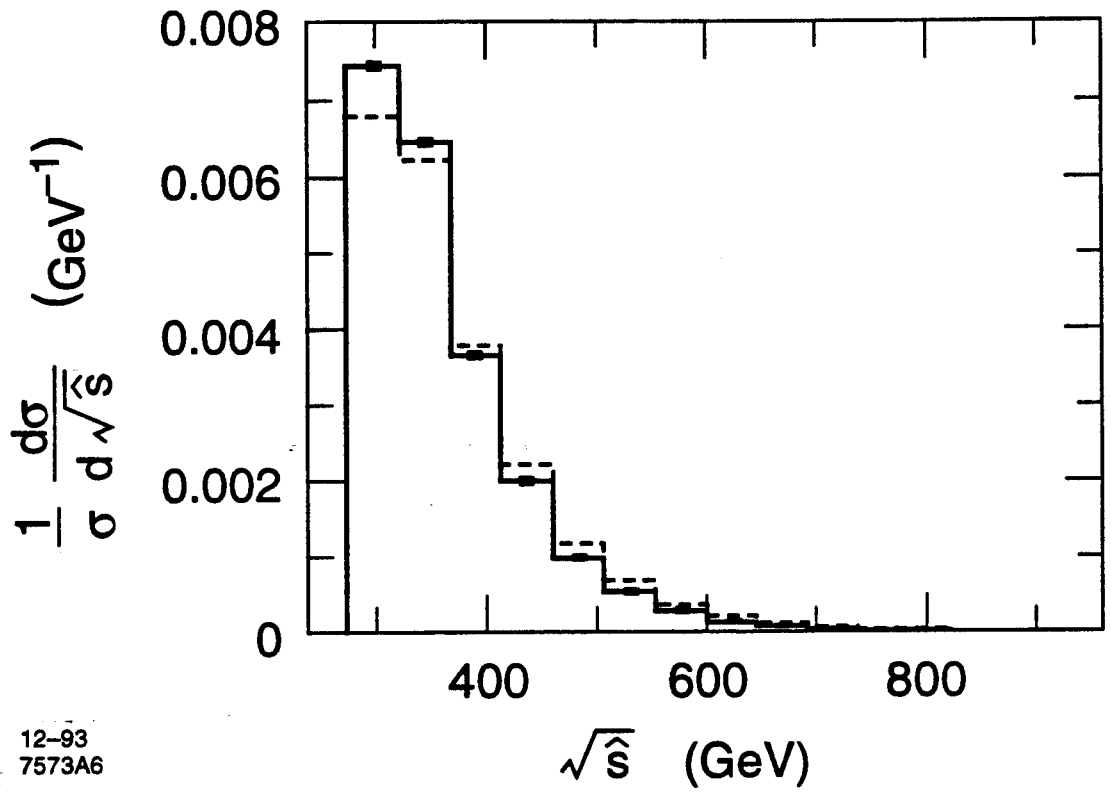


Fig. 2c

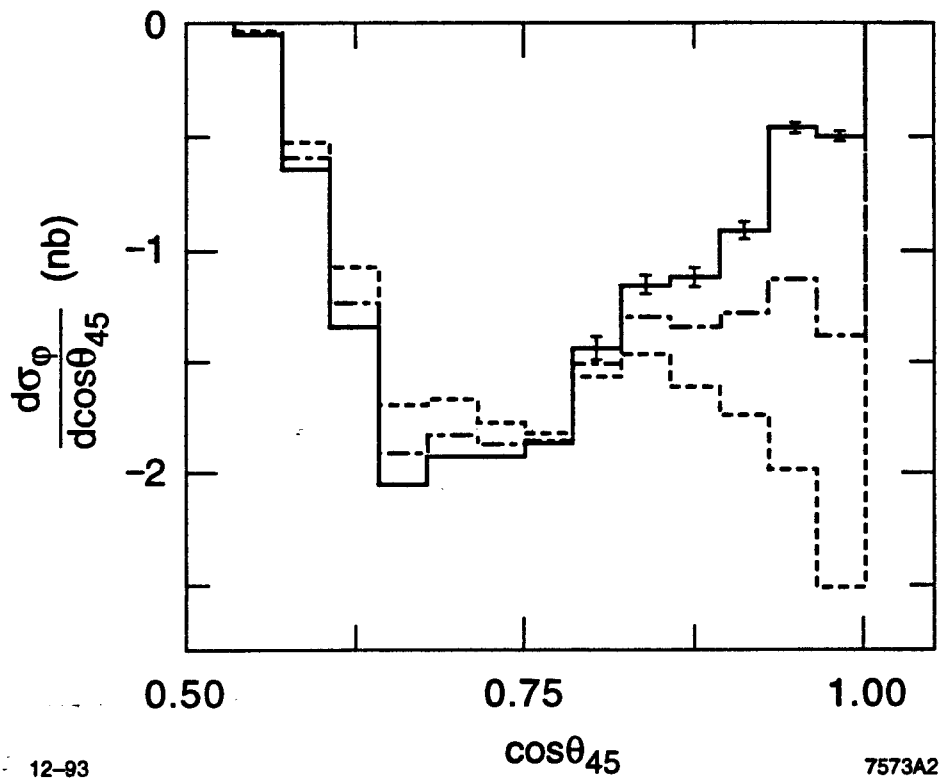
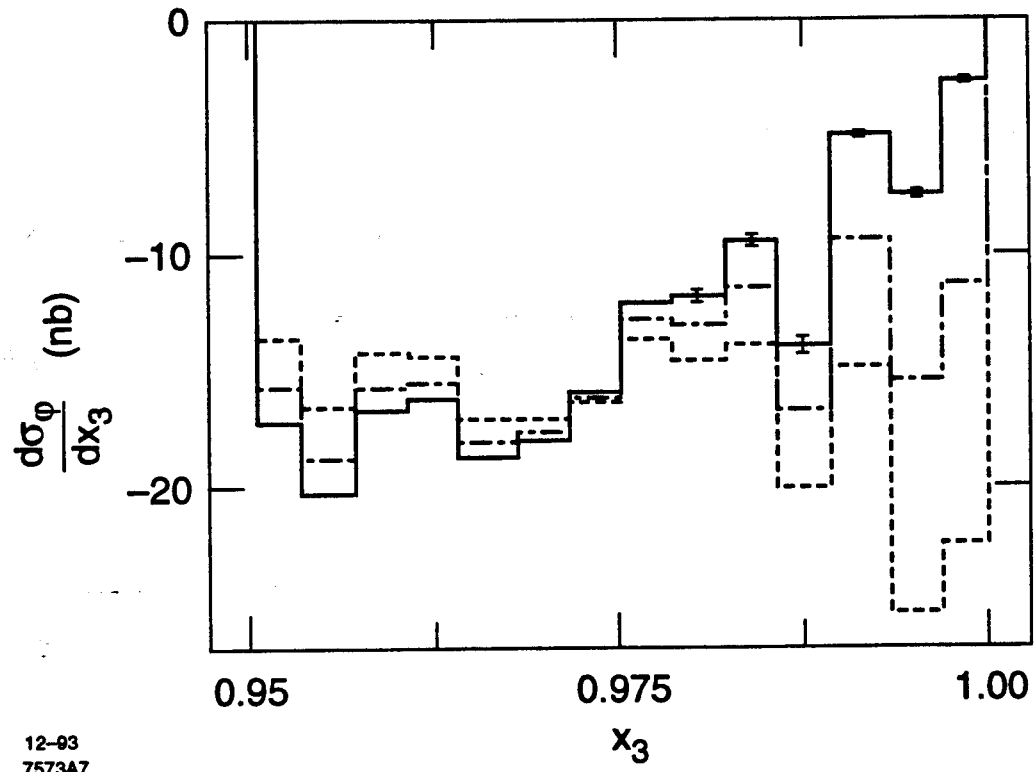


Fig. 3a



12-83
7573A7

Fig. 3b

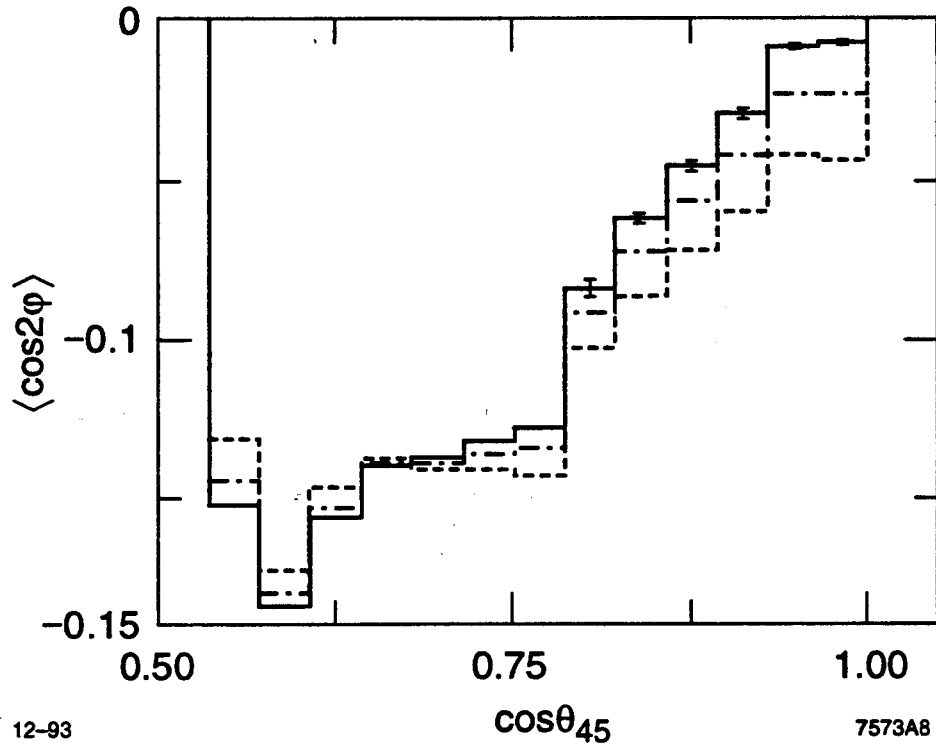


Fig. 3c

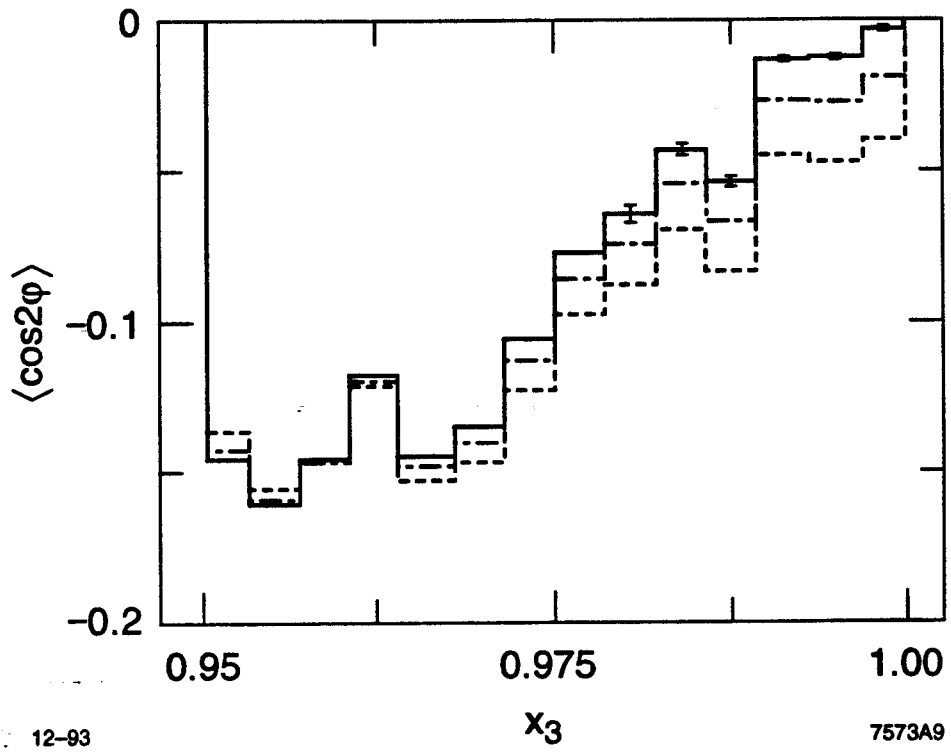


Fig. 3d

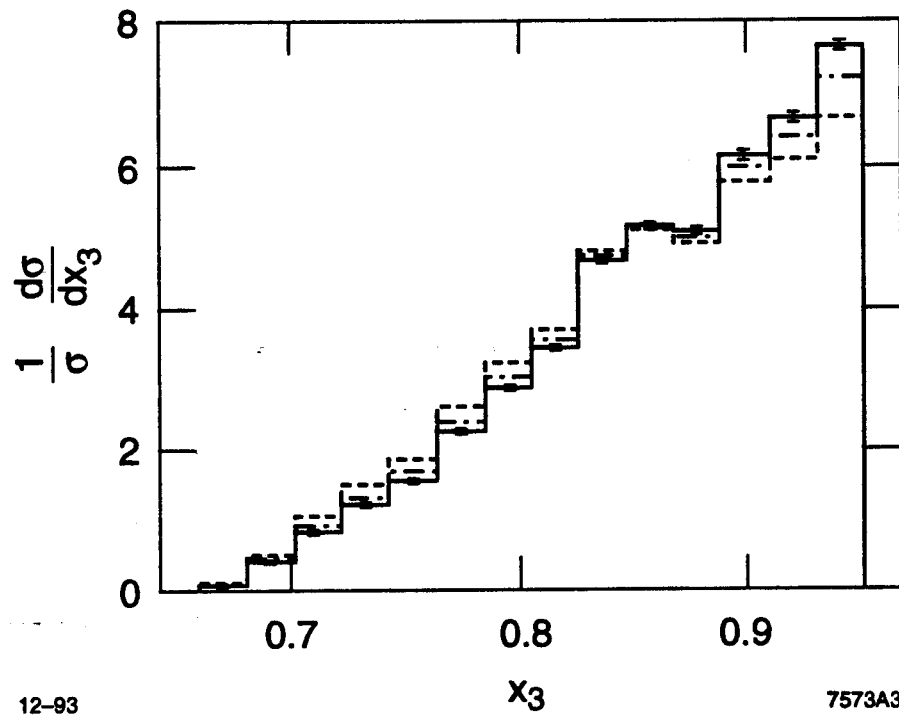
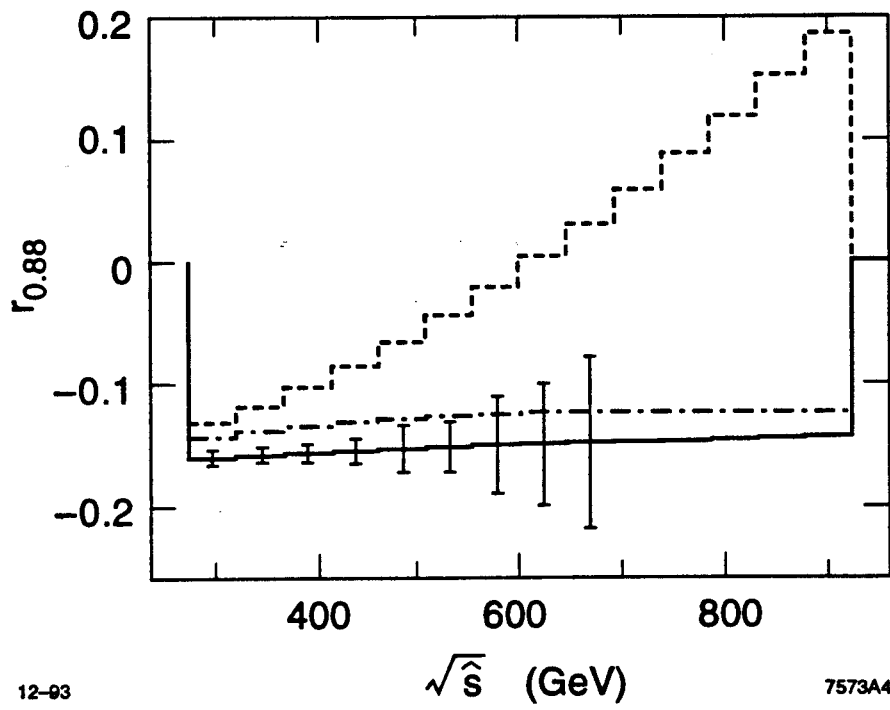


Fig. 4



12-93

7573A4

Fig. 5